Introducing time dependent dynamics in modeling the implied volatility surface

MSc Thesis

ERASMUS UNIVERSITY
ERASMUS SCHOOL OF ECONOMICS
ECONOMETRIC INSTITUTE

ORTEC FINANCE

Author:
Mike van der Houwen
Studentnumber: 323437
Start: February 2012
End: August 2012

Supervisors:
Prof. Dr. D. van Dijk
Dr. K.M. Lee

Co-reader:
Dr. M. van der Wel

August 12, 2012

Abstract

The purpose of this study was to investigate whether introducing time dependent surface dynamics would improve the modeling of implied volatility surfaces. The aim of the research is therefore to see whether models which incorporate these dynamics perform better than a benchmark model, currently used at ORTEC Finance to model option price scenarios, that uses an implied volatility surface with a constant shape, of which a single point is modeled over time.

Three different models are used; principal component analysis, the Heston model and a regression model based on terms which are functions of moneyness and maturity. All three models and the benchmark model are calibrated on the implied volatility surface at the end of each month in the period January 2005 till June 2012, for both the Standards & Poor 500 (SPX index) and the Euro Stoxx 50 (SX5E index). Afterwards the calibrated parameters that follow from these models are modeled over time using regression models. These regression models are mostly AR(1) models with additional independent variables like the return of the SPX index, realized volatility, VIX index or the consumer price index. A final comparison of the performance of these models is made in terms of the mean absolute error over time and surface.

Two of the three models are an improvement over the benchmark model in modeling the implied volatility surfaces of both the SPX index and the SX5E index. The Heston model is only a slight improvement over the benchmark model, while the regression model shows better improvements. The regression models contains five terms; a constant, moneyness divided by the square root of maturity, moneyness squared divided by maturity, maturity and moneyness times the square root of maturity. The principal component analysis shows an almost constant mean absolute error, which is higher than the mean absolute error of the other models (and also the benchmark model). Since two of the three models that allow the shape of the volatility surface to change over time are an improvement over the benchmark model, it can be concluded that introducing time dependent surface dynamics does improve the modeling of implied volatility surfaces.

Samenvatting

Het doel van deze studie is het onderzoeken of door het introduceren van tijdsafhankelijke oppervlakte dynamieken het modelleren van implied volatiliteit oppervlakken wordt verbeterd. Daarom wordt in dit onderzoek bekeken of modellen die deze dynamiek bevatten beter presteren dan een benchmark model dat een implied volatiliteit oppervlakte gebruikt met een constante vorm, waarvan een enkel punt wordt gemodelleerd over tijd.

Drie verschillende modellen worden gebruikt; principale componenten analyse, het Heston model en een regressie model gebaseerd op termen die functies zijn van moneyness en looptijd. Alle drie de modellen en het benchmark model zijn gekalibreerd op implied volatiliteit oppervlakken aan het eind van elke maand in de periode januari 2005 tot juni 2012, voor zowel de Standards & Poor 500 (SPX index) als de Euro Stoxx 50 (SX5E index). Daarna zijn de gekalibreerde parameters, die volgen uit deze modellen, gemodelleerd over de tijd met regressie modellen. Deze regressie modellen zijn grotendeels AR(1) modellen met extra onafhankelijke variabelen zoals het rendement van de SPX index, gerealiseerde volatiliteit, VIX index of de consumenten prijs index. Een vergelijking in prestatie van deze modellen wordt gemaakt in termen van gemiddelde absolute fout in implied volatiliteit over tijd en oppervlakte.

Twee van de drie modellen blijken een verbetering te zijn ten op zichten van het benchmark model in het modelleren van implied volatiliteit oppervlakken voor zowel de SPX als de SX5E index. Het Heston model laat een kleine verbetering zien, terwijl het regressie model een grotere verbetering laat zien. Het regressie model bestaat uit vijf termen; een constante, moneyness gedeeld door de wortel van de looptijd, moneyness kwadraat gedeeld door de looptijd, de looptijd en moneyness keer de wortel van de looptijd. Principale componenten analyse resulteert in een bijna constante gemiddelde absolute fout in implied volatiliteit over tijd, welke hoger is dan de gemiddelde absolute fout van de andere modellen (ook het benchmark model). Omdat twee van de drie modellen die de vorm van het implied volatiliteit oppervlakte laten veranderen over tijd een verbetering is ten opzichte van het benchmark model, kan geconcludeerd worden dat door het introduceren van tijdsafhankelijke oppervlakte dynamiek wel het modelleren van implied volatiliteit oppervlakten wordt verbeterd.

Contents

Abstract iii

Samenvatting v

Contents vii

1 Introduction 3

2 Literature 5
- 2.1 Implied volatility surface 5
- 2.2 Regression models 6
- 2.3 Heston model 7
- 2.4 ORTEC model 7

3 Data 9

4 Methodology 11
- 4.1 Principal Component Analysis 11
- 4.2 Regression models 12
- 4.3 Heston model 12
  - 4.3.1 Heston model derivation 12
    - SVJ 14
    - SVJJ 14
    - Feller condition 14
  - 4.3.2 COS method 15
    - Fourier integrals and cosine series 15
    - Pricing European options 16
    - Heston Model in COS 17
    - Truncation 17
  - 4.3.3 Calibration 18
- 4.4 Regression models for parameters over time 18

5 Results 19
- 5.1 Principal Component Analysis 19
  - 5.1.1 Time series of components scores 22
    - SPX 22
    - SX5E 25
- 5.2 Regression models 26
  - 5.2.1 Calibration 26
  - 5.2.2 Time series of parameters 27
    - SPX 28
    - SX5E 31
- 5.3 Heston 33

5.3.1 SVJ Model 33
5.3.2 Calibration 33
Unrestricted parameters 33
Restricted parameters 36
5.3.3 Time series of parameters 36
SPX 36
SX5E 39
5.4 Benchmark: ORTEC Model 41
5.4.1 Time series of reference point 41
5.5 Comparison 44
5.5.1 After calibration 44
5.5.2 Final comparison 46

6 Conclusion **51**
6.1 Recommendations 52

Acknowledgements **55**

Bibliography **57**

A Appendix **61**
A.1 Average Skew IV Surface 62
A.2 Regression Model 3: Reduction in R squared 63
A.3 Terms of Regression Model 3 64
A.4 Worst and best fits 65
A.4.1 SPX 65
Benchmark 65
Heston 66
PCA 67
Regression 68
A.4.2 SX5E 69
Benchmark 69
Heston 70
PCA 71
Regression 72

CHAPTER 1

Introduction

A measure for the uncertainty of the returns provided by stock is the volatility, σ (Hull (2012)). Historical volatility is the standard deviation of the underlying price of the asset over a historical period. Next to historical volatility, literature uses the implied volatility. The most used implied volatility, is the one which follows from the famous formula of Black and Scholes (1973). Christensen and Prabhala (1998) state that the implied volatility is widely regarded as the option market's forecast of future return volatility over the remaining life of the relevant option. Some research indicate that the implied volatility is a good predictor of the realized volatility (Jorion (1995), Beckers (1981), Chiras and Manaster (1978), Giot (2003)), although other research indicate that the implied volatility is a biased predictor of future realized volatility (Lamoureux and Lastrapes (1993), Day and Lewis (1992), Canin and Figlewski (1993)).

Lee (2002) explains Black-Scholes implied volatility as a language used to express the price of an option. Many traders use the implied volatility to compare the values of options with different underlyings, strikes and maturities. This means implied volatility is not only used as a predictor of future volatility, its main use is to price options of different underlyings, strikes and maturities. To model the implied volatility surface therefore means to model the prices of sets of options. Improvements in these models lead to having a better idea of the returns and risks of options.

Under the Black-Scholes model the implied volatility of an option is constant over maturity and moneyness. However, when the implied volatilities of different maturity and moneyness combinations are calculated from market data, the implied volatility varies across maturity and moneyness. An implied volatility surface can be constructed if one has the implied volatility of options with different maturity and moneyness. The level and shape of the implied volatility surface change over time.

In available literature about modeling implied volatilities time series, usually only one implied volatility is modeled over time. For example the Chicago Board Options Exchange Market Volatility Index (VIX) is a popular measure of the implied volatility of S&P 500 index options and is the variable to be modeled. The dependency of implied volatility on maturity and moneyness is not taken into account.

There are models available in literature from which the volatility surface can be constructed, the most well-known being the model of Heston (1993). These models are not time dependent and from them one can construct the volatility surface at one certain time step. This means that there are not many methods to model the implied volatility surface in time. The Heston model is the most well-known and popular of all stochastic volatility models (Gatheral (2006)).

There are not many scientific papers on the time dependent dynamics of the implied volatility surface. Historical data show that the shape of the implied volatility surface is not constant over time. It is therefore relevant to investigate possible time dependent dynamics of the implied volatility surface and to construct ways to model the implied volatility surface, instead of only one implied volatility.

Thesis goal

At ORTEC Finance the implied volatility surface is kept constant by using the historical implied volatility surface relative to one reference point, which is modeled over time. ORTEC Finance constructs scenarios for a wide range of economic and financial variables, used by institutional investors to support ALM analyses, asset allocations and risk studies. In reality the market data shows that the shape of the implied volatility surface is not constant over time. The main motivation for this thesis is to improve the modeling of the implied volatility surface by incorporating a dynamic surface over time, so that it can be used in the dynamic scenario generator (DSG), which uses a large dynamic factor model to construct multivariate scenarios for economic and financial variables. The implied volatilities are used to price options. Better scenarios from the DSG lead to better predictions in Asset Liability Management studies, which are used by pension funds and insurance companies.

The idea behind this thesis is to develop a way to model the implied volatility surface, including time dependent surface dynamics. The research question for thesis is therefore:

Does introducing time dependent surface dynamics improve models of the implied volatility surface?

Three models that are able to capture time dependent surface dynamics of the implied volatility surface will be compared to a benchmark model with an implied volatility surface shape which does not change over time. The first model is based on principal component analysis, for which the first two or three principal component scores will be modeled over time. The second model is the Heston model, for which the parameters will be modeled over time. While both models are already used in literature to model implied volatility surface, the modeling of the component scores / parameters is a new contribution to literature. The third model is a regression model, which uses terms like moneyness and maturity to describe an implied volatility surface. Afterwards the coefficients of the regression model are modeled over time. There is some literature available which uses principal component analysis on the coefficients of such a regression model, and afterwards models the component scores over time using autoregressive models. In this thesis the coefficients of the regression model themselves are modeled over time. All models are more thoroughly explained in Chapter 2 and 4.

Structure of the report

The second chapter of this thesis is a brief overview of available literature. The Heston model, ORTEC's model and various regression models are described. The third chapter gives an explanation of the data that is used in this thesis.

The fourth chapter outlines the methods that are used in this thesis. The models mentioned in the literature review are explained more thoroughly. Also the use of principal component analysis and the COS method is outlined. The fifth chapter contains all results and is also a comparison between the model of ORTEC and the various models described in this thesis.

The final chapter of this thesis contains the conclusions and recommendations for future work.

CHAPTER 2

Literature

In this section various literature is reviewed. First some literature is given which explains the implied volatility surface. Then various literature describing regression models on the implied volatility surface are discussed. Afterwards literature on the Heston model is discussed. Finally a summary is given of the model that is currently used at ORTEC Finance.

2.1 Implied volatility surface

The uses of implied volatility are already discussed in Chapter 1. The implied volatility is calculated by using the famous formula of Black and Scholes (1973) and Merton (1973). To calculate the value of an option, Black and Scholes (1973) assume that the asset price S_t follows a log normal process with constant volatility σ, along with other assumptions like no transaction costs, that the option is a European option and that the underlying asset pays no dividends. The value of a call option c and put option p are given by (Hull (2012)):

$$c = S_0 N(d_1) - K e^{-r\tau} N(d_2), \tag{2.1}$$

$$p = K e^{-r\tau} N(-d_2) - S_0 N(-d_1), \tag{2.2}$$

$$d_1 = \frac{\ln\left(\frac{S_0}{K}\right) + \left(r + \frac{\sigma^2}{2}\right)\tau}{\sigma\sqrt{\tau}}, \tag{2.3}$$

$$d_2 = \frac{\ln\left(\frac{S_0}{K}\right) + \left(r - \frac{\sigma^2}{2}\right)\tau}{\sigma\sqrt{\tau}}, \tag{2.4}$$

where $N(x)$ is the cumulative probability distribution function for a standardized normal distribution, S_0 is the current index level, K is the exercise price or strike price, τ is the time to maturity and r is the risk-free interest rate.

If one has the above information, including the price of a call or put option, it is possible to calculate the implied volatility, which is the volatility implied by the Black-Scholes-Merton model. Although the Black-Scholes model implicates a constant implied volatility across strike price and maturity, when the implied volatilities are calculated for options of the same underlying asset for different maturities and strike prices, the implied volatility tends to differ across strike price and maturity. Using the implied volatility of different maturity and strike price combinations, it is possible to construct the implied volatility surface. Usually the term moneyness is used instead of strike prices. Moneyness is defined as the strike price divided by the spot price.

The most important shapes that can be seen in the implied volatility surface are the volatility skew and volatility smile (Brigo and Mercurio (2002)). Peña et al. (1999) explain that the implied volatility appears to be different across strike prices and Kamal and Gatheral (2010) state that the since the 1987 stock market crash, implied volatility surfaces have been characterized by the volatility skew. The volatility skew refers to the phenomenon that the trend that for a given expiration date, the implied volatilities increase when the strike price decreases for strike prices below the spot price. For short maturities the implied volatility surface has the shape of a V across strike prices, this is also called the volatility smile. Peña et al. (1999) state that the volatility smile indicates that the Black-Scholes formula tends to misprice deep in-the-money and deep out-of-the-money options.

Instead of using the implied volatility from the Black-Scholes formula, model-free implied volatility indices have been created. The VIX index is a measure of the average level of the implied volatility surface (Simon (2003)). Ahoniemi (2008) state that the most widely followed index is the VIX index, calculated by the Chicago Board Options Exchange from S&P 500 index option prices. Simon (2003) explains the VIX index as an investor 'fear index'. Extreme values of the VIX index can be seen as trading signals. When the VIX index is very high, markets are pessimistic, which leads to a period of sustained increases in stock prices. For extreme low levels of the VIX index the market is set up for disappointment and the odds of a downward market correction are raised. How the VIX index is calculated is explained in Chapter 3.

2.2 Regression models

Some researchers proposed to model the implied volatility surface at a specific moment in time using a multiple regression model. In these regression models the implied volatility depends on independent variables which are functions of moneyness and maturity. Alentorn (2004) proposed three regression models, the first representing a constant volatility, the second being able to capture the volatility smile across moneyness and the third model also adds effects of maturity and a combined effect of maturity and moneyness. A fourth extension was added by Badshah (2009). The fourth model includes a way to capture the time to maturity curvature effect. The models are given below:

$$\sigma(m,\tau,t) = \beta_{0,t} + \varepsilon, (M1) \tag{2.5}$$

$$\sigma(m,\tau,t) = \beta_{0,t} + \beta_{1,t}M + \beta_{2,t}M^2 + \varepsilon, (M2) \tag{2.6}$$

$$\sigma(m,\tau,t) = \beta_{0,t} + \beta_{1,t}M + \beta_{2,t}M^2 + \beta_{3,t}\tau + \beta_{4,t}M\tau + \varepsilon, (M3) \tag{2.7}$$

$$\sigma(m,\tau,t) = \beta_{0,t} + \beta_{1,t}M + \beta_{2,t}M^2 + \beta_{3,t}\tau + \beta_{4,t}M\tau + \beta_{5,t}\tau^2 + \varepsilon, (M4) \tag{2.8}$$

where σ is the implied volatility, M is a function of the moneyness m and maturity τ(see Chapter 3) and ε an error term. Alentorn (2004) found the best results with the third model, which captures the smile across moneyness and the term structure across time to expiration. Badshah (2009) found that, both model 3 and 4, perform better than the one dimensional smile model.

Roux (2007) proposed another parametric model of the volatility surface. The model of Roux (2007) is as follows:

$$\sigma(m,\tau,t) - \mathrm{VIX}_t = a_{0,t} + a_{1,t}\log m + a_{2,t}\frac{1}{\sqrt{\tau}} + a_{3,t}(\log m)^2 + a_{4,t}\frac{\log m}{\sqrt{\tau}} + a_{5,t}\frac{(\log m)^2}{\sqrt{\tau}} (M5) \tag{2.9}$$

where m is the strike price divided by the current spot price (moneyness). The model is motivated by a few empirical observations. The first being that if implied volatility is plotted as a function of the logarithm of m, it tends to have a parabolic shape. The second observation is that if the implied volatilities for a given strike are plotted against one over the square root of the maturity time, the shape tends to be linear. The least squares procedure is used to estimate the model parameters. Instead of minimizing the sum of the squared errors, a weighting scheme is used. The weight is the actual observed value of implied volatility.

The model of Roux (2007) gives six parameters for every time step. Using principal component analysis (PCA), the six parameters are reduced to two or three components. These principal components are modeled using autoregressive processes of the form:

$$k_{i,t} = \alpha_i k_{i,t-1} + \beta_i \varepsilon_{i,t} \tag{2.10}$$

where $k_{i,t}$ is the i-th principal component at time t.

A benchmark regression model is the Practitioners Black Scholes model by Christoffersen and Jacobs (2004), also known as the ad-hoc model of Dumas et al. (1998). It is a more simpler version of the above models. It contains the following terms:

$$\sigma(m,\tau,t) = B_{0,t} + B_{1,t}m + B_{2,t}m^2 + B_{3,t}\tau + B_{4,t}\tau^2 + B_{5,t}m\tau, (PBS) \tag{2.11}$$

where again m is strike price divided by the current spot price (moneyness) and τ is the maturity in years. In the original paper the strike price was used instead of the moneyness, but at every time step there is simply a constant factor between the strike price and moneyness. The Practitioners Black Scholes model was used by Christoffersen and Jacobs (2004) in a paper that stresses the importance of the loss function in option valuation. It states that when models are compared, they should be based on the same loss functions (e.g. relative or absolute sum of squared errors). If this is not the case, inappropriate comparison will be made.

2.3 Heston model

Heston (1993) derived a closed-form solution for the price of a European call option on an asset with stochastic volatility. The Heston model is used to model option prices, from which implied volatilities can be constructed. The Heston model has five parameters, the mean reversion rate κ, the long term variance θ, the initial variance V_0, volatility of variance η and correlation parameter ρ.

The Heston models assumes that the spot asset at time t follows the diffusion process given below:

$$dS(t) = \mu S dt + \sqrt{V(t)} S dW_1(t), \tag{2.12}$$

where $W_1(t)$ is a Wiener process. The Heston model also includes a stochastic volatility process given by:

$$dV(t) = \kappa \left[\theta - V(t)\right] dt + \eta \sqrt{V(t)} dW_2(t), \tag{2.13}$$

where $W_2(t)$ is another Wiener process. $W_1(t)$ and $W_2(t)$ are correlated with correlation coefficient ρ.

Guo (1998) applied the Heston model to PHLX currency options prices. He regressed the future variance on the variance based on the Heston model, variance based on the White and Hull model and historical variance. Whenever the Heston variance was present, the other variables played no role. Lin et al. (2001) found that the Heston model was an improvement over the Black-Scholes model, using FTSE 100 index options as a test case. Fiorentini et al. (2002) used the Heston model in a thinly traded market, the Spanish IBX 35 index. Their findings are that the Heston model tends to overprice the out-of-the-money options and underprice the in-the-money options. Also, the correlation coefficients are very volatile. Aboura (2003) compared the Heston model with the White and Hull model for French PXL European call options. While the overall pricing performance of the models is the same, Heston's model tends to perform better at short term and deep-out-the-money calls. Bin (2007) did daily calibrations with the Heston model and found that both the correlation coefficient and the mean reversion rate are volatile.

Bates (1996) proposed an extension of the Heston model. This extension consists of a jump in the stochastic volatility model. This jump might explain why the skew of short expirations is so steep and why the short-dated term structure of skew is inconsistent with any stochastic volatility model (Gatheral (2006)).

More details about the Heston model can be found in Sec. 4.3 in the methodology chapter.

2.4 ORTEC model

Equity implied volatilities are implemented as regression variables depending on log returns of the underlying index, realized volatility and lagged implied volatilities. The implied volatility of the 12 month, ATM (100% moneyness) option is modeled. All other combinations of moneyness and maturity are based on the historical implied volatility surface with the 12 month maturity, 100% moneyness implied volatility as a reference point. The regression model:

$$\mathrm{IV}_t = \alpha + \sum_i \beta_i \mathrm{RV}_{t-i} + \sum_j \gamma_j \mathrm{Ret}_{t-j} + \sum_k \delta_k \mathrm{IV}_{t-k} + u_t, \qquad u_t \sim \mathrm{IID}(0, \sigma^2), \tag{2.14}$$

where IV_t, RV_t and Ret_t are the implied volatility (100% moneyness and 12 month maturity), the realized volatility and the return of the underlying asset at time t, respectively.

Afterwards skew tables (containing multiplication factors with the reference point, the 12 month, ATM implied volatility) are used to calculate the implied volatilities of the other points (80% - 120% moneyness and maturity of 1, 2, 3, 6, 18, 24 months). This means that the relative shape of the historical implied volatility surface is kept constant over time and only the level is changed.

CHAPTER 3

Data

The data that are necessary for this research includes an implied volatility surface at different time steps (months, more specific the last trading day of each month). For this research the implied volatility surface of the Standards & Poor 500 (SPX index) and the Euro Stoxx 50 (SX5E index) is used. Daily data is available in Bloomberg from January 2005 till June 2012 for the SPX index, while for the SX5E index the data is available from January 2006 till June 2012. All implied volatility surfaces consist of sixtythree points. The implied volatility is given for nine different values of moneyness and seven different maturities, see table 3.1 for a summary. For some combinations the data is only available from sixth month of 2005. The implied volatility surface of November 2010 of both the SPX and SX5E index is shown in Fig. 3.1. For the SX5E index the 80% and 120% moneyness implied volatilities are only available from November 2010 and onwards.

The mean level of the surfaces fluctuates around 0.20 with 0.10 and 0.45 as low and high peaks, respectively. Some surfaces show the volatility smile, while all surfaces show that implied volatility of in-the-money options tend to be higher than the implied volatility of out-of-the-money options. The highest IV is 0.69/0.68, at the highest maturity and moneyness, and the lowest IV is 0.7/0.10, at the highest maturity and lowest moneyness for the SPX/SX5E implied volatility surface. For low moneyness the implied volatility tends to decrease with higher maturity, while for high moneyness the implied volatility tends to increase with higher maturity.

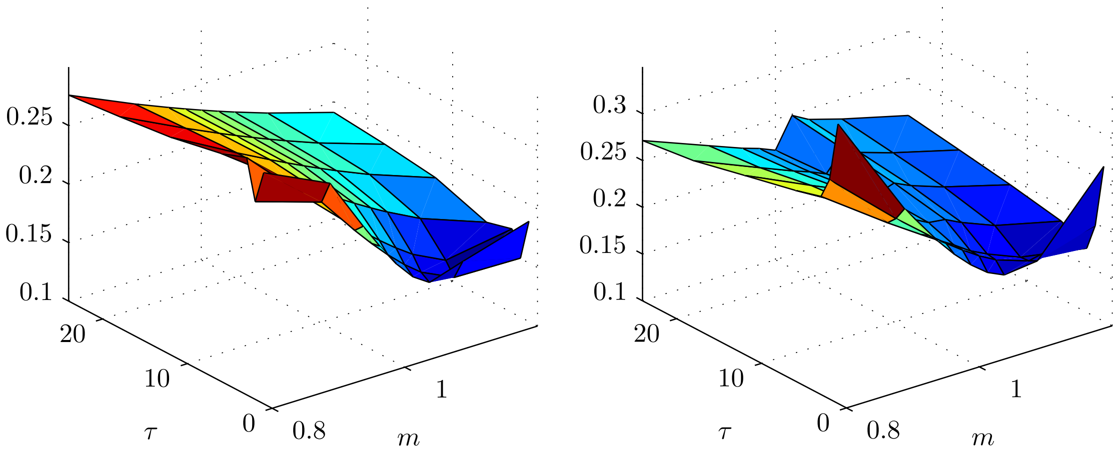

Figure 3.1: Implied volatility surface at the end of November 2010 of the SPX index (left) and SX5E index (right), respectively. For every month an implied volatility surface can be constructed.

Moneyness m is the strike price divided by the spot price, this is also the definition used by Bloomberg. In some papers, e.g. Badshah (2009), a different definition is used for moneyness. The definition that is used in Badshah (2009) is:

$$M = \frac{\log\left(\frac{S}{Ke^{-r\tau}}\right)}{\sqrt{\tau}}, \tag{3.1}$$

Date	January 2005 - June 2012
Moneyness	80%, 90%, 95%, 97.5%, 100%, 102.5%, 105%, 110%, and 120%
Maturity	1, 2, 3, 6, 12, 18 and 24 months

Table 3.1: Implied volatilities data summary

where K is the strike price, S the spot price, τ the maturity and r the risk free rate. In this thesis the Bloomberg definition of moneyness will be used. The other moneyness definition, denoted as M, is only used to explain the regression model by Badshah (2009). In this thesis for the regression model of Badshah the risk free rate term will be taken out of the definition.

The risk free rate is necessary as an input of the Black-Scholes formula and Heston model. For the risk-free rate the following tickers in Bloomberg will be used for the 1 year maturity and 2 year maturity, respectively: *USSA1* and *USSA2*. For the risk-free rate in the calibration of the SX5E index the following tickers will be used for the 1 year and 2 year, respectively: *EUSA1* and *EUSA2*.

Other variables that are used in the regressions are the monthly returns of the indices and the realized volatility. The realized volatility of one month is computed from the daily returns of the indices in that month, using the following formula:

$$RV = \sqrt{12 \sum_{\#\text{ Days}} r^2}, \tag{3.2}$$

where r is the daily return of index.

The VIX index, a model-free volatility measure, is available in Bloomberg and is calculated using the two nearest expiration months of S&P 500 call and put options, Exchange (2003). More information about the VIX index is given in Sec. 2.1. The calculation of the VIX index is done as follows:

$$\text{VIX} = 100\sqrt{\frac{2}{T}\sum_i \frac{\Delta K_i}{K_i^2} e^{rT} Q(K_i) - \frac{1}{T}\left[\frac{F}{K_0} - 1\right]^2}, \tag{3.3}$$

where T is the time to expiration of the option contract, F is the forward index level derived from option prices, K_i is the strike price of the i$^{\text{th}}$ out-of-the-money option, ΔK_i the difference between the strike prices, K_0 is the first strike price below F, r is the risk-free interest rate up to the expiration of the option contract and $Q(K_i)$ is the midpoint of the bid-ask spread for each option with strike price K_i. The VIX index is calculated using implied volatilities of only short maturities. The V2X is a similar index for the European market.

CHAPTER 4

Methodology

This chapter includes various methods that will be applied in this thesis. First the principal component analysis is explained. Secondly the regression models are given. Finally, the Heston model and the benchmark are outlined.

4.1 Principal Component Analysis

Principal component analysis (PCA) is applied to the 63/49 time series of implied volatilities of fixed moneyness and maturity combinations. This results in a reduced number of components which are able to capture most of the variance in the 63/49 time series. The component scores of these limited number of components are modeled using regression models. The problem with this method is that only a limited number of points on the volatility surface is predicted. Only the fixed moneyness and maturity combinations are predicted, other points will have to be interpolated.

Principal component analysis was first introduced by Pearson (1901). In PCA the variance in n variables is described by a reduced number of components k ($k \leq n$), which explain as much variance as possible. PCA uses eigenvalue decomposition of the correlation matrix to find component scores and loadings. A detailed explanation of PCA is given in Jolliffe (2002).

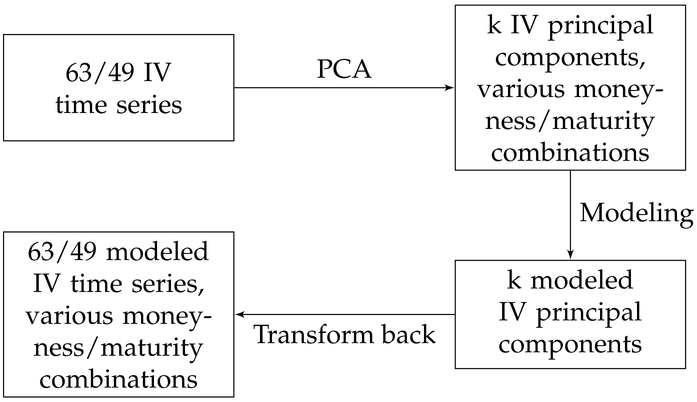
63/49 IV time series
PCA
k IV principal components, various moneyness/maturity combinations
Modeling
k modeled IV principal components
Transform back
63/49 modeled IV time series, various moneyness/maturity combinations

Figure 4.1: Flow diagram of modeling the IV surface with PCA method.

4.2 Regression models

The various regression models given in Chapter 2 are calibrated for every time step. This results in time series of the parameters in the regression models, for which models will be constructed. An advantage over the PCA model is that the implied volatility can be calculated of options which have moneyness and maturity combinations which are different from the ones observed in the market data. Afterwards one regression model is chosen for which the parameters will be modeled over time using regression models.

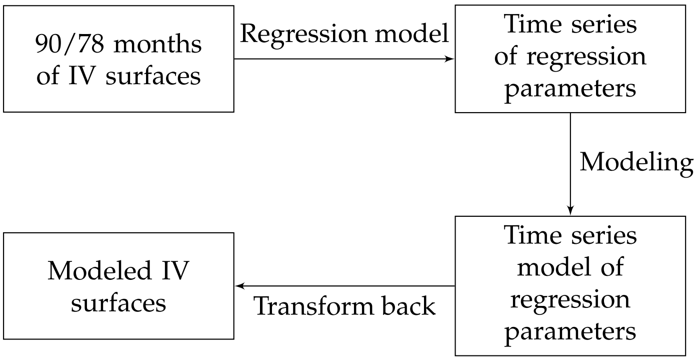
90/78 months of IV surfaces
Regression model
Time series of regression parameters
Modeling
Time series model of regression parameters
Transform back
Modeled IV surfaces

Figure 4.2: Flow diagram of modeling the IV surface with regression model method.

4.3 Heston model

The Heston model is calibrated for every time step, resulting in time series of the five parameters of the Heston model. Afterwards time series are constructed of these parameters. Variables that are used are the historical implied volatilities/VIX index, realized volatilities and return of the underlying asset (the SPX index). The calibration procedure of the Heston model is explained in Sec. 4.3.3.

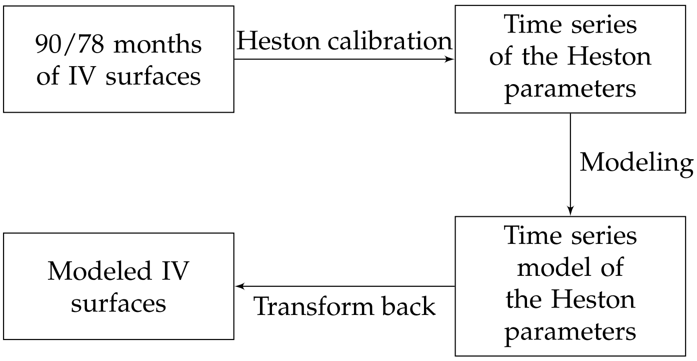
90/78 months of IV surfaces
Heston calibration
Time series of the Heston parameters
Modeling
Time series model of the Heston parameters
Transform back
Modeled IV surfaces

Figure 4.3: Flow diagram of modeling the IV surface with the Heston method.

4.3.1 Heston model derivation

The derivation of the Heston model starts from the assumption that the spot asset at time t follows the diffusion process given below:

$$dS(t) = \mu S(t)dt + \sqrt{V(t)}S(t)dW_1(t), \tag{4.1}$$

where $W_1(t)$ is a Wiener process. The volatility follows a diffusion process as well:

$$dV(t) = \kappa\left[\theta - V(t)\right]dt + \eta\sqrt{V(t)}dW_2(t), \tag{4.2}$$

where $W_2(t)$ is another Wiener process. $W_1(t)$ and $W_2(t)$ are correlated with correlation coefficient ρ.

Assuming a constant interest rate r the price at time t of a unit discount bond that matures at time $t + \tau$ is given by:

$$P(t, t+\tau) = e^{-r\tau}. \tag{4.3}$$

Heston (1993) shows that standard arbitrage arguments show that the value of any asset $U(S, \nu, t)$ must satisfy the following partial differential equation:

$$\frac{1}{2} V S^2 \frac{\partial^2 U}{\partial S^2} + \rho \eta V S \frac{\partial^2 P_j}{\partial S \partial V} + \frac{1}{2} \eta^2 V \frac{\partial^2 U}{\partial V^2} + r S \frac{\partial U}{\partial S} + \left(\kappa \left[\theta - V(t)\right] - \lambda(S, V, t)\right) \frac{\partial U}{\partial V} - rU + \frac{\partial U}{\partial t} = 0, \tag{4.4}$$

where $\lambda(S, V, t)$ is the price of volatility risk.

Fiorentini et al. (2002) found that the price of volatility risk is not significantly different from zero, and therefore has no effect. In this thesis it is assumed that the price of volatility risk is zero. This reduces the number of parameters from six to five.

A European call option, an option which can only be executed at the maturity date, with strike price K and maturing at time T is constricted by the following boundary conditions:

$$\begin{aligned} U(S, V, T) &= \text{Max}(0, S \cdot K), \\ U(0, V, t) &= 0, \\ \frac{\partial U}{\partial S}(\infty, V, t) &= 1, \\ rs \frac{\partial U}{\partial S}(S, 0, t) + \kappa\theta \frac{\partial U}{\partial V}(S, 0, t) - rU(S, 0, t) + U_t(S, 0, t) &= 0, \\ U(S, \infty, t) &= S. \end{aligned} \tag{4.5}$$

In analogy with the Black-Scholes formula, Heston (1993) guessed a solution in the following form:

$$C(S(t), V(t), \tau) = S(t) P_1 - K e^{-r\tau} P_2 \tag{4.6}$$

where the two terms stand for the present value of the spot asset upon optimal exercise and the present value of the strike-price payment, respectively. Both terms in the above equation must satisfy the partial differential equation given in Eq. (4.4). Substituting Eq. (4.6) in Eq. (4.4) leads to:

$$\frac{1}{2} V \frac{\partial^2 P_j}{\partial x^2} + \rho \eta V \frac{\partial^2 P_j}{\partial x \partial V} + \frac{1}{2} \eta^2 V \frac{\partial^2 P_j}{\partial V^2} + (r + u_j V) \frac{\partial P_j}{\partial x} + (a - b_j V) \frac{\partial P_j}{\partial V} + \frac{\partial P_j}{\partial t} = 0, \tag{4.7}$$

for $j = 1, 2$, where:

$$u_1 = \tfrac{1}{2}, \quad u_2 = -\tfrac{1}{2}, \quad a = \kappa\theta, \quad b_1 = \kappa + \lambda - \rho\eta, \quad b_2 = \kappa + \lambda. \tag{4.8}$$

The option price needs to satisfy the boundary conditions given in Eq. (4.5) and therefore the principal differential equations must satisfy:

$$P_j(x, V, T; \ln[K]) = 1_{x \geq \ln[K]}, \tag{4.9}$$

where $x = \ln S$. P_1 and P_2 can be interpreted as risk-neutralized probabilities (Cox and Ross (1976)). P_j is the conditional probability that the option expires in-the-money. These probabilities are not available in closed form. However, Heston (1993) derived characteristic functions that satisfy the partial differential equations given in Eq. (4.4). The probabilities can be derived from these characteristic functions. The final integrand used to calculated P_j and all needed functions, including characteristic Heston function

f_j are given below:

$$\begin{aligned}
P_j &= \frac{1}{2} + \frac{1}{\pi}\int_0^{\infty} \mathrm{Re}\left[\frac{e^{-i\phi \ln K + i\phi x} f_j}{i\phi}\right] d\phi. && (4.10)\\
f_j &= e^{C_j + D_j \nu} && (4.11)\\
C_j &= r\phi i\tau + \frac{a}{\eta^2}\left((b_j - \rho\eta\phi i + d)\,\tau - 2\ln\left[\frac{1 - ge^{d\tau}}{1-g}\right]\right) && (4.12)\\
D_j &= \frac{b_j - \rho\eta\phi i + d}{\eta^2}\left[\frac{1 - e^{d\tau}}{1 - ge^{d\tau}}\right] && (4.13)\\
g_j &= \frac{b_j - \rho\eta\phi i + d}{b_j - \rho\eta\phi i - d} && (4.14)\\
d_j &= \sqrt{\left(\rho\eta\phi i - b_j\right)^2 - \eta^2\left(2u_j\phi i - \phi^2\right)} && (4.15)
\end{aligned}$$

SVJ

Bates (1996) proposed an extension of the Heston model consisting of a jump in the stochastic volatility model. Wilmott (2007) assumes that stochastic volatility model with jumps (SVJ) is given by:

$$dS(t) = \mu S(t)dt + \eta S(t)dW_1 + (e^{\alpha + \delta\epsilon} - 1)S(t)dq, \tag{4.16}$$

where $\epsilon \sim N(0,1)$ and dq is a Poisson process given by:

$$dq = \begin{cases} 0 & \text{with probability 1-}\lambda_J \\ 1 & \text{with probability } \lambda_J \end{cases} \tag{4.17}$$

This means that the SVJ model has three additional paramaters, compared to the normal Heston model. The new parameters are α, mean jump, δ, jump variance, and λ_J, probability of occurence of jump. In case of jumps the characteristic function also changes. The characteristic function of the Heston model is multiplied by the jump characteristic function (Gatheral (2003)):

$$f_{\text{Jump}} = e^{-i\phi\lambda_J T\left(e^{\alpha + \frac{\delta^2}{2}} - 1\right) + \lambda_J T\left(e^{i\alpha\phi - \phi^2\frac{\delta^2}{2}} - 1\right)}. \tag{4.18}$$

SVJJ

Jumps in stock prices are often followed by jumps in volatility. SVJJ models are able to deal with these kind of jumps. An example is the model of Matytsin (1999). A disadvantage of the SVJJ model is the additional number of parameters. Since in this thesis there is a limited number of data available of implied volatilities the SVJJ model will not be considered. It is too difficult to calibrate SVJJ models with only a limited amount of data, Nilsson (2008).

Feller condition

If the correlation coefficient is between -1 and 1, and the other four parameters are positive, the stochastic volatility can not become zero when the Feller condition is satisfied (Albrecher et al. (2006)). The Feller condition is given by:

$$2\kappa\theta > \eta^2. \tag{4.19}$$

The calibration procedure, explained in Section 4.3.3, obtains worse fits when the Feller condition needs to be met. The restriction of the Feller condition will therefore not be used. The calibrated volatilities are not zero anywhere, which means the region where the volatility can possibly be zero is not the region studied in this thesis.

4.3.2 COS method

Calibration is a big issue in the Heston model. Many local minima are present when trying to find the five parameters. Fang and Oosterlee (2008) developed an option pricing method for European options based on the Fourier-cosine series, called the COS method. This method can be applied to calculate the Heston model, and therefore also used for calibration of the Heston model. The COS method shows impressive speed compared to other techniques (e.g. Carr and Madan (1999)).

Fourier integrals and cosine series

Fang and Oosterlee (2008) starts the derivation of the COS method with the risk-neutral valuation formula for pricing European options:

$$v(x,t_0) = e^{-r\Delta t}\mathbb{E}^{\mathbb{Q}}[v(y,T)|x] = e^{-r\Delta t}\int_{\mathbb{R}} v(y,T)f(y|x)dy, \tag{4.20}$$

where v is the option value, Δt is the difference between the maturity T and the initial date t_0, $\mathbb{E}^{\mathbb{Q}}[\cdot]$ is the expectation operator under risk-neutral measure $\mathbb{Q}$, x and y are state variables at time t_0 and T, respectively. Finally, $f(y|x)$ is the probability density of y given x and r is the risk-free interest rate.

A closed form expression for the integral is available in Fourier space. Fang and Oosterlee (2008) uses the FFT algorithm to return to the time domain. The probability density and its characteristic functions form a Fourier pair, given by:

$$\phi(\omega) = \int_{\mathbb{R}} e^{ix\omega} f(x)dx \tag{4.21}$$

$$f(x) = \frac{1}{2\pi}\int_{\mathbb{R}} e^{-ix\omega}\phi(\omega)d\omega \tag{4.22}$$

Equation (4.22) includes the inverse Fourier integral, which can be solved using its Fourier-cosine series expansion, extracting the series coefficients directly from the integrand.

A function in the domain $[0,\pi]$, has the following cosine expansion series:

$$f(\theta) = {\sum_{k=0}^{\infty}}' A_k \cdot \cos(k\theta), \tag{4.23}$$

where $\sum'$ indicates that the first term of the summation is weighted by a half and the coefficients A_k are given by

$$A_k = \frac{2}{\pi}\int_0^{\pi} f(\theta)\cos(k\theta)d\theta. \tag{4.24}$$

Functions supported in a different interval, e.g. $[a,b] \in \mathbb{R}$, can easily be mapped on the domain $[0,\pi]$ by using the following transformations:

$$\theta = \frac{x-a}{b-a}\pi, \tag{4.25}$$

$$x = \frac{b-a}{\pi}\theta + a. \tag{4.26}$$

Equation (4.23) and Eq. (4.24) can therefore be rewritten to:

$$f(x) = {\sum_{k=0}^{\infty}}' A_k \cdot \cos\left(k\frac{x-a}{b-a}\pi\right), \tag{4.27}$$

$$A_k = \frac{2}{b-a}\int_a^b f(x)\cos\left(k\frac{x-a}{b-a}\pi\right)dx. \tag{4.28}$$

Any real function has a cosine expansion when it it finitely supported. A Fourier transform can only exist when the integrands in Eq. (4.22) decay to zero at $\pm\infty$, and therefore a and b can be low finite numbers without losing accuracy. They can be chosen in such a way that:

$$\phi_1(\omega) = \int_a^b e^{i\omega x} f(x)dx \approx \int_{\mathbb{R}} e^{i\omega x} f(x)dx = \phi(\omega). \tag{4.29}$$

A_k can now rewritten to:

$$A_k = \frac{2}{b-a}\text{Re}\left[\phi_1\left(\frac{k\pi}{b-a}\right) \cdot e^{\left(-i\frac{ka\pi}{b-a}\right)}\right], \tag{4.30}$$

where Re $[\cdot]$ stands for the real part of the argument. Together with Eq. (4.29) it follows that $A_k \approx F_k$, where F_k is given by:

$$A_k = \frac{2}{b-a}\text{Re}\left[\phi\left(\frac{k\pi}{b-a}\right) \cdot e^{\left(-i\frac{ka\pi}{b-a}\right)}\right]. \tag{4.31}$$

Using the above approximation Eq. (4.27) can be rewritten in terms of F_k:

$$f_1(x) = {\sum_{k=0}^{\infty}}' F_k \cos\left(k\pi\frac{x-a}{b-a}\right). \tag{4.32}$$

Since the Fourier terms decay to zero at $\pm\infty$ the series can be truncated:

$$f_2(x) = {\sum_{k=0}^{N-1}}' F_k \cos\left(k\pi\frac{x-a}{b-a}\right). \tag{4.33}$$

The difference between $f_2(x)$ and $f(x)$ is an error because of the approximation of A_k by F_k and a truncation error from going to $f_1(x)$ to $f_2(x)$.

According to Boyd (2001) cosine series expansion of entire functions, functions without singularities, exhibits an exponential convergence. The series can therefore be used for highly accurate approximations with no singularities on the domain $[a, b]$.

Pricing European options

The risk-neutral valuation formula for pricing European options given in the Eq. (4.20) can now be rewritten to:

$$v_1(x, t_0) = e^{-r\Delta t}\int_a^b v(y, T) f(y|x)dy. \tag{4.34}$$

Since the characteristic function is known, while the probability density function is not, the probability density function is replaced by its cosine series:

$$f(y|x) = {\sum_{k=0}^{\infty}}' A_k(x) \cos\left(k\pi\frac{y-a}{b-a}\right), \tag{4.35}$$

where

$$A_k(x) = \frac{2}{b-a}\int_a^b f(y|x) \cos\left(k\pi\frac{y-a}{b-a}\right) dy. \tag{4.36}$$

The risk-neutral valuation formula can now again be rewritten, filling in Eq. (4.35) in Eq. (4.34) results in:

$$v_1(x, t_0) = e^{-r\Delta t}\int_a^b v(y, T){\sum_{k=0}^{\infty}}' A_k(x) \cos\left(k\pi\frac{y-a}{b-a}\right) dy. \tag{4.37}$$

Fang and Oosterlee (2008) include a new definition,

$$V_k = \frac{2}{b-a}\int_a^b v(y, T) \cos\left(k\pi\frac{y-a}{b-a}\right) dy, \tag{4.38}$$

which is used to rewrite the risk-neutral valuation formula again to:

$$v_1(x,t_0) = \frac{1}{2}(b-a)e^{-r\Delta t} \cdot {\sum_{k=0}^{\infty}}' A_k(x)V_k. \tag{4.39}$$

Finally, this formula can be truncated and $A_k(x)$ can be replaced by $F_k(x)$ which results in:

$$v(x,t_0) \approx e^{-r\Delta t} {\sum_{k=0}^{N-1}}' \mathrm{Re}\left[\phi\left(\frac{k\pi}{b-a};x\right)e^{-ik\pi\frac{a}{b-a}}\right]V_k. \tag{4.40}$$

Heston Model in COS

Fang and Oosterlee (2008) found a way to simplify Eq. (4.40) in case of a Heston model. The formula then looks like:

$$v(\mathbf{x},t_0,u_0) \approx \mathbf{K}e^{-r\Delta t} \cdot \mathrm{Re}\left[{\sum_{k=0}^{N-1}}' \varphi_{hes}\left(\frac{k\pi}{b-a};u_0\right)U_k \cdot e^{ik\pi\frac{x-a}{b-a}}\right], \tag{4.41}$$

where u_0 is the initial volatility of the underlying, $\mathbf{K}$ is a vector of strike prices, φ_{hes} is the characteristic function of the log-asset price in the Heston model given by:

$$\varphi_{hes}(\omega;u_0) = e^{i\omega\mu\Delta t + \frac{\mu_0}{\eta^2}\left(\frac{1-e^{-D\Delta t}}{1-Ge^{-D\Delta t}}\right)(\lambda - i\rho\eta\omega - D)} \cdot e^{\frac{\lambda\bar{v}}{\eta^2}\left(\Delta t(\lambda - i\rho\eta\omega - D) - 2\log\left(\frac{1-Ge^{-D\Delta t}}{1-G}\right)\right)}, \tag{4.42}$$

where D and G are given by:

$$D = \sqrt{(\lambda - i\rho\eta\omega)^2 + (\omega^2 + i\omega)\eta^2}, \tag{4.43}$$

$$G = \frac{\lambda - i\rho\eta\omega - D}{\lambda - i\rho\eta\omega + D}. \tag{4.44}$$

U_k is derived from the coefficients for Plain Vanilla, Digital and Gap options in Fang and Oosterlee (2008). It is given by:

$$U_k = \begin{cases} \frac{2}{b-a}(\chi_k(0,b) - \phi_k(0,b)) & \text{for a call,} \\ \frac{2}{b-a}(-\chi_k(0,b) + \phi_k(0,b)) & \text{for a put.} \end{cases} \tag{4.45}$$

where $\chi_k(c,d)$ and $\psi_k(c,d)$ are given by:

$$\psi_k(c,d) = \frac{1}{1+\left(\frac{k\pi}{b-a}\right)^2}\left[\cos\left(k\pi\frac{d-a}{b-a}\right)e^d - \cos\left(k\pi\frac{c-a}{b-a}\right)e^c\right. \tag{4.46}$$

$$\left. + \frac{k\pi}{b-a}\sin\left(k\pi\frac{d-a}{b-a}\right)e^d - \frac{k\pi}{b-a}\sin\left(k\pi\frac{c-a}{b-a}\right)e^c\right] \tag{4.47}$$

$$\chi_k(c,d) = \begin{cases} \left[\sin\left(k\pi\frac{d-a}{b-a}\right) - sin\left(k\pi\frac{c-a}{b-a}\right)\right]\frac{b-a}{k\pi} & k \neq 0 \\ (d-c) & k = 0 \end{cases} \tag{4.48}$$

Truncation

Fang and Oosterlee (2008) use the following range for $[a,b]$:

$$[a,b] = [c_1 - 12\sqrt{|c_2|}, c_1 + 12\sqrt{|c_2|}], \tag{4.49}$$

where c_1 and c_2 are given by:

$$c_1 = \mu T + (1 - e^{-\lambda T})\frac{\bar{u} - u_0}{2\lambda} - \frac{1}{2}\bar{u}T \tag{4.50}$$

$$\begin{aligned} c_2 = &\frac{1}{8\lambda^3}\left[\eta T\lambda e^{-\lambda T}(u_0 - \bar{u})(k\lambda\rho - 4\eta) + \lambda\rho\eta(1 - e^{-\lambda T})(16\bar{u} - 8u_0)\right. \\ &\left. + 2\bar{u}\lambda T(-4\lambda\rho\eta + \eta^2 + 4\lambda^2) + \eta^2((\bar{u} - 2u_0)e^{-2\lambda T} + \bar{u}(6e^{-\lambda T} - 7) + 2u_0) + 8\lambda^2(u_0) - \bar{u})(1 - e^{-\lambda T})\right]. \end{aligned} \tag{4.51}$$

Since calculating c_1 and c_2 takes up a lot of computational time, an arbitrary a and b can be chosen which are always higher than the given range in Eq. (4.49). This way the integral takes a bit longer to be calculated, but time is saved by not having to calculate both Eq. (4.50) and Eq. (4.51).

4.3.3 Calibration

To calibrate the Heston parameters for one implied volatility surface the following steps are made. First all implied volatilities on the implied volatility surface are translated to prices using the Black-Scholes formula (Market price). Secondly, using the COS method for every combination of the five Heston parameters, moneyness, maturity and risk-free rate the price (COS price) can be calculated. The standard MATLAB minimizing function *fmincon* (Matlab) is used to find five Heston parameters for which the quadratic errors between the market price and COS price is as low as possible. Since there are many local minima, hundreds of random starting points are used to finally obtain a good minima.

If five Heston parameters are known, the implied volatility surface can be calculated by first calculating the prices (COS price) of all maturity/moneyness combinations. Afterwards the Black-Scholes formula is used to obtain the implied volatility surface.

4.4 Regression models for parameters over time

The models for parameters over time are mostly AR models, with additional independent variables. These variables can be macroeconomic variables like the consumer price index or gross domestic product. The mostly used independent variables are the VIX/V2X index and the returns of the SPX/SX5E index. Next to the well known t-test for the significance of each variable, three tests are performed for every model. These tests are the Ljung-Box test, Breusch-Pagan test and Jarque-Bera test.

The Ljung-Box test (Ljung and Box (1978)) is used to see whether there is autocorrelation in the residuals of the regression model. The null hypothesis of the test is 'The data are serially correlated', while the alternative hypothesis is 'The data are not serially correlated'. Under the null hypothesis the JB-statistic has a chi-square distribution with 5 degrees of freedom, since the test is applied to autocorrelation over 5 lags.

The Breusch-Pagan test (Breusch and Pagan (1979) is used to see whether the residuals are heteroskedastic. The null hypothesis of the test is 'The residuals are homoskedastic', while the alternative hypothesis is 'The residuals are heteroskedastic'. Under the null hypothesis the LM-statistic has a chi-square distribution with k degrees of freedom, where k is the number of independent variables used in the regression.

The Jarque-Bera test (Jarque and Bera (1987) is used to see whether the residuals are normally distributed. The null hypothesis is therefore 'The residuals are normally distributed', while the alternative hypothesis is 'The residuals are not normally distributed'. Under the null hypothesis the JB-statistic has a chi-square distribution with 2 degrees of freedom. Sometimes after omitting the largest error the JB test can no longer reject the null hypothesis. In these cases the JB statistic with omitting the x largest error will be given in the results table as JB/(x).

CHAPTER 5

Results

This chapter is arranged in five different parts. First the results of the principal components are shown. The variance explained by the first few components are shown and the regression models for the components scores are given. The second part shows the results of the regression models. The time series of the regression parameters are given, including models for these time series. The third part consists of the results of the Heston model. Also included are the models for the time series of the Heston parameter. In the fourth part the results of the ORTEC Model, the benchmark, are shown. In the final part of the results, all models are compared with the benchmark model.

5.1 Principal Component Analysis

In principal component analysis the number of variables is reduced to a limited number of components. For this thesis there are sixty-three variables, which are all time series of implied volatility for different moneyness/maturity combinations. For the SX5E index, the 80% moneyness and 120% moneyness data are only available from the year 2010 and onwards, therefore these moneyness combinations will be left out of the PCA analysis. For the SX5E index there are fourty-nine variables.

Table 5.1 contains the variance and cumulative variance explained by the first few components. For both the SPX index and the SX5E, component one already explains 95% of the variance, which indicates that there are high correlations between the different time series. The second component explains more than 2% of the variance. The third component only explains 1% and 0.5% for the SPX index and SX5E index, respectively. Higher components explain even less and will therefore not be used in the further analysis.

Component	Variance explained (%)		Cumulative variance explained (%)	
	SPX	SX5E	SPX	SX5E
1	94.89	96.32	94.89	96.32
2	2.66	2.24	97.55	98.56
3	1.07	0.45	98.62	99.01
4	0.51	0.29	99.13	99.29
5	0.40	0.20	99.53	99.49
6	0.17	0.14	99.70	99.63
7	0.09	0.11	99.78	99.74

Table 5.1: This table shows the variance explained and cumulative variance explained by the first seven principal components. The number of variables is sixty three and forty nine for the SPX IV surface and SX5E IV surface, respectively.

To construct an implied volatility surface from the first two components, the loadings of these components are needed and the average implied volatility surface. The average implied volatility surface, loadings (illustrated as a surface) of the first, second and third component of both the SPX index and the SX5E index are shown in Fig. 5.1 and Fig. 5.2. The averaged implied volatility surfaces clearly show a smile across moneyness at the 1 month maturity. At longer maturities the average implied volatility surface of the SPX index is smooth and decreases with moneyness, while the average implied volatility surface is less smooth for the SX5E index. The smile across moneyness remains in the surface even for higher maturities.

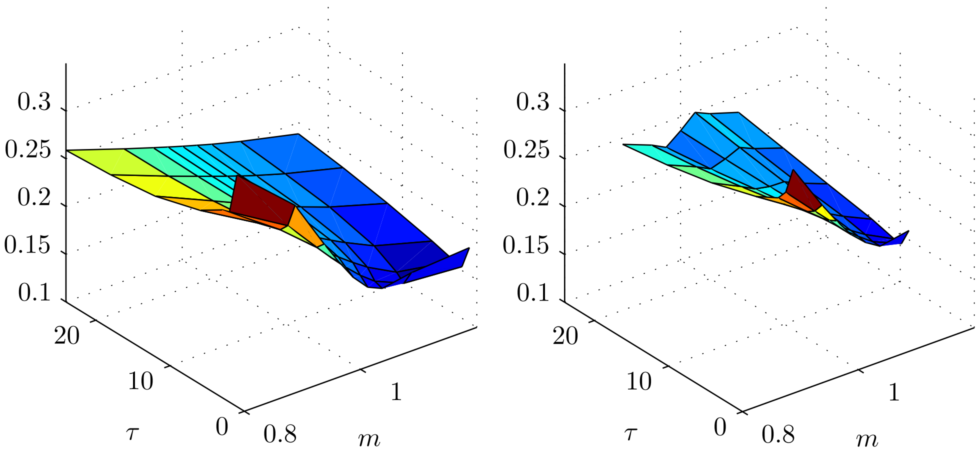

Figure 5.1: The average implied volatility surface of the SPX index (left) and the SX5E index (right).

The first and second components of both the SPX and SX5E surface are quite similar, not taking into account the smile across moneyness for higher maturities of the SX5E index. The loadings of the first components seem to have an opposite smile across moneyness for shorter maturities. The loadings slightly decrease for longer maturities. Because all loadings of the first components are positive, this can be seen as a level factor. The loadings of the second components decrease a lot with higher maturity. The second component can be seen as a maturity factor, since it mostly differs across maturities. Again the loadings for longer maturities are smooth for the SPX index, while they are not for the SX5E index.

The third component of the SPX index and the SX5E index are not similar. The third component of the SPX index has a smile across moneyness for short maturities and has positive loadings in-the-money while, the loadings are negative out-of-the-money. It can therefore be seen as a moneyness factor. The third component of the SX5E index has a smile across moneyness over the entire surface. For the SX5E index the loadings are actually positive out-of-the-money and negative in-the-money.

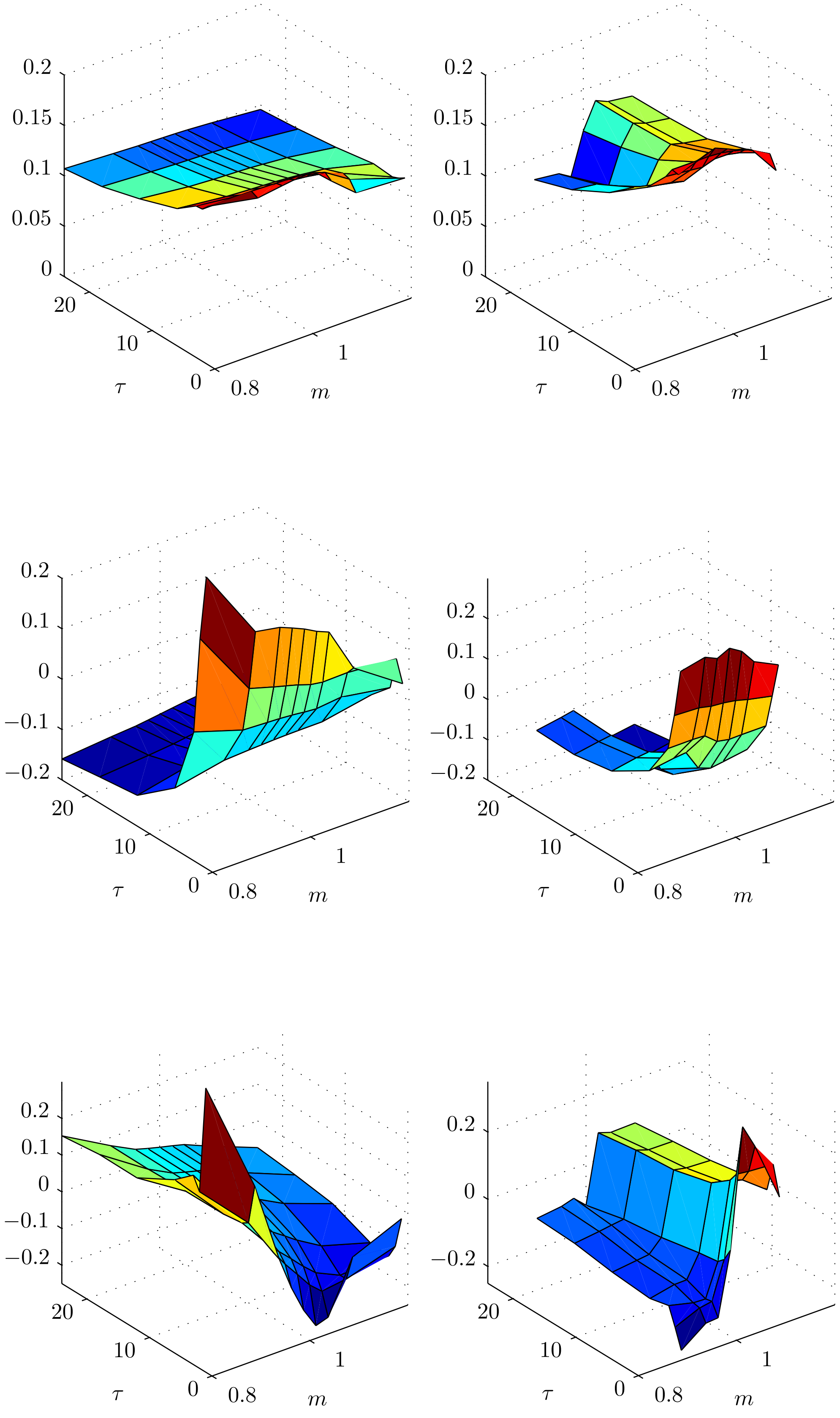

Figure 5.2: The loadings of the first (top), second component (middle) and third component (bottom) for the SPX index (left) and the SX5E index (right).

5.1.1 Time series of components scores

The component scores of the first three components need to be modeled, so that the modeled implied volatility surface can be constructed every month. The scores of the first two principal components of the SPX index are shown in Fig. 5.3. The first components of SPX index and the SX5E index is highly correlated with the VIX index (0.99) and V2X index (0.99), respectively. The second component of both indices is more volatile. For both indices the second component is uncorrelated with the VIX (V2X) index (0.11). There is however some correlation with the realized volatility and returns of the underlying indices. The second component of the SPX index has a correlation coefficient of 0.25 with the realized volatility and -0.39 with the returns of the underlying index. The second component of the SX5E index has a correlation coefficient of 0.30 with the realized volatility and -0.42 with the returns of the underlying index. There is some autocorrelation, with the first lag it is 0.61 and 0.51 for the SPX index and SX5E index, respectively.

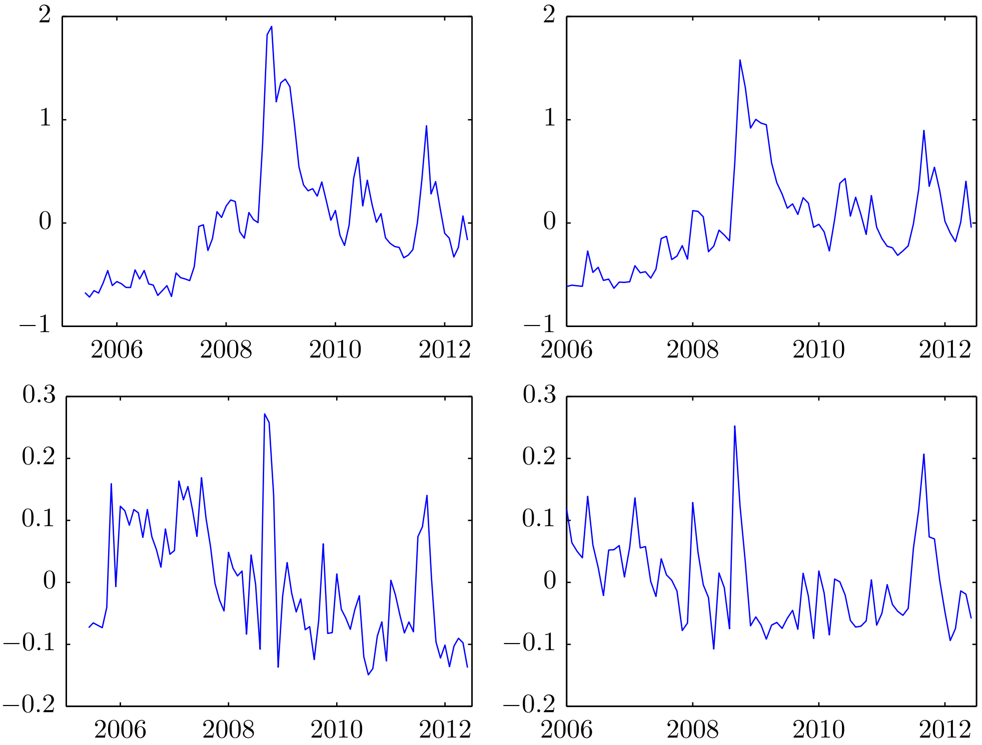

Figure 5.3: The first component (top) and second component (bottom) for the SPX index (left) and SX5E index (right).

SPX

The regression models for the principal components are AR(1) models with additional independent variables such as macroeconomic variables. The first principal component has a very high correlation with the VIX index, therefore the VIX index will be used as an independent variable as well. The addition of the US Treasury bill yield (3-month) increases the performance of the regression model. The results of the regression are shown in Table 5.2. The regression model accounts for almost 99% of the variance in the first component. The Ljung-Box test shows that there is no significant autocorrelation in the errors, while the Breusch-Pagan test shows that the errors are not heteroskedastic. The Jarque-Bera shows that the errors are not normally distributed, but after the removal of two outliers the null hypothesis of normally distributed can not be rejected. In Table 5.2 the JB/(2) statistic is basically the Jarque-Bera test done after omitting the two largest errors. The first component enhances the level of the surface. Since the VIX index consists of a weighted average of the implied volatility of options with various moneyness and maturity combinations it makes sense that the VIX index has a positive effect on the first principal component. The US treasy bill yield (3-month) has a negative effect on the first principal component, which means that a high US treasury bill yield means a lower implied volatility surface. The variable with the largest influence on the level of the implied volatility surface remains however the VIX index.

Dependent variable: PCA1 (SPX Index)

Variable	Coefficient	Std. Error	t	p	Part. R^2
C	-0.9670	0.0301	-32.09	0.00	0.9287
$PCA1_{t-1}$	0.2108	0.0235	8.98	0.00	0.5054
VIX_t	4.4478	0.1241	35.83	0.00	0.9420
$TBSR_t$ (US)	-1.1761	0.4342	-2.71	0.01	0.0850
R^2	0.9895		LB	$\chi^2(5)=3.71$ [0.592]	
Adj. R^2	0.9891		LM	$\chi^2(3)=1.91$ [0.591]	
N	83		JB	$\chi^2(2)=120.51$ [0.000]	
Std. Error	0.0608		JB/(2)	$\chi^2(2)=2.61$ [0.271]	

Table 5.2: Regression results of the first component of PCA, PCA2. (SPX Index).

For the second component the first lag of the second component is used, as well as the returns of the SPX index and the nominal government long term bond (10y) yield (NGLR). The results, shown in Table 5.3, indicate that almost 60% of the variance in the second component can be explained by the regression model. Again the homoskedasticty and no autocorrelation hypotheses can not be rejected. After the removal of the two largest errors, the hypothesis of normally distributed errors can not be rejected. The second principal component has influence on how the surface is shaped across maturity. If the second principal component is positive the implied volatility at higher maturities will be increased, while the implied volatility at lower maturities will be decreased. A negative second principal component will increase the implied volatility at lower maturities and decrease the implied volatility at higher maturities. The returns have a negative impact on the second principal component, while the nominal government long term bond yield has a positive effect on the second principal component.

Dependent variable: PCA2 (SPX Index)

Variable	Coefficient	Std. Error	t	p	Part. R^2
C	-0.1377	0.0312	-4.42	0.00	0.1982
PCA_{t-1}	0.3958	0.0828	4.78	0.00	0.2244
Ret_t	-0.7014	0.1432	-4.90	0.00	0.2328
$NGLR_t$ (US)	3.8704	0.8438	4.59	0.00	0.2103
R^2	0.5873		LB	$\chi^2(5)=3.49$ [0.625]	
Adj. R^2	0.5716		LM	$\chi^2(3)=3.15$ [0.369]	
N	83		JB	$\chi^2(2)=20.61$ [0.000]	
Std. Error	0.0632		JB/(1)	$\chi^2(2)=1.94$ [0.378]	

Table 5.3: Regression results of the second component of PCA, PCA2. (SPX Index).

The regression model of the third principal component includes one lag and the returns of the SPX index as independent variables. The model explains more than 60% of the variance in the third principal component. All null hypotheses can not be rejected (no autocorrelation, homoskedastic errors, normal distrubtion of errors). The third principal component has the largest effect accross moneyness. A positive third principal component increases the implied volatility of in-the-money options while decrease the implied volatility of out-of-the-money options. There is also a smile across moneyness in the third principal component for lower maturities. The returns of the SPX index have a positive effect on the third principal component.

Dependent variable: PCA3 (SPX Index)

Variable	Coefficient	Std. Error	t	p	Part. R^2
C	0.0025	0.0040	0.62	0.54	0.0047
$PCA3_{t-1}$	0.7276	0.0655	11.11	0.00	0.6066
Ret_t	0.1314	0.0826	1.59	0.12	0.0307
R^2	0.6183		LB	$\chi^2(5)$=4.17 [0.526]	
Adj. R^2	0.6088		LM	$\chi^2(2)$=5.58 [0.061]	
N	83		JB	$\chi^2(2)$=0.19 [0.909]	
Std. Error	0.0367		-	-	

Table 5.4: Regression results of the third component of PCA, PCA3. (SPX Index).

SX5E

Just as the first principal component of the SPX index, the first principal component of the SX5E index has a very high correlation with an implied volatility index, the V2X index. As regressors the one month lag of the first principal component is used, together with the V2X index and also the one month lag of the V2X index. The model explains more than 99% of the variance in the first principal component. Since the V2X is positively correlated with the first principal component and it has the biggest partial R^2 its coefficient is positive. There tends to be some overshooting, since the one month lag of the V2X index has a negative coefficient.

Dependent variable: PCA1 (SX5E Index)

Variable	Coefficient	Std. Error	t	p	Part. R^2
C	-0.6939	0.1010	-6.87	0.00	0.3959
$PCA1_{t-1}$	0.4938	0.0756	6.53	0.00	0.3722
$V2X_t$	4.4676	0.0899	49.69	0.00	0.9717
$V2X_{t-1}$	-1.8210	0.3920	-4.65	0.00	0.2306
R^2	0.9927		LB	$\chi^2(5)$=10.05 [0.074]	
Adj. R^2	0.9924		LM	$\chi^2(3)$=3.96 [0.266]	
N	76		JB	$\chi^2(2)$=0.60 [0.740]	
Std. Error	0.0413		-	-	

Table 5.5: Regression results of the first component of PCA, PCA1. (SX5E Index).

The second principal component of the SX5E index has the same effect as the second principal component of the SPX index. A positive second principal component increases the implied volatility at lower maturities and decreases the implied volatility at higher maturities. Together the one month lag of the second principal component, the returns of the SX5E index, the indirect real estate total return index, the SX5E index and one month lag of the SX5E index are able to explain more than 55% of the variance in the second principal component. The null hypothesis of normally distributed errors can only be rejected if the two largest errors are removed. Both the returns of the SPX5e index and indirect real estate total return index have a positive coefficient. The coefficient of the SX5E index is negative, but there is a lot of overshooting since the coefficient of the one month lag of the SX5E index is positive and almost of the same magnitude.

Dependent variable: PCA2 (SX5E Index)

Variable	Coefficient	Std. Error	t	p	Part. R^2
C	-0.0323	0.0263	-1.23	0.22	0.0210
$PCA2_{t-1}$	0.4035	0.0834	4.84	0.00	0.2505
Ret_t	0.8081	0.4629	1.75	0.08	0.0417
$INRE_t$ (EU)	0.0004	0.0001	3.65	0.00	0.1598
$SX5E_t$	-0.0005	0.0002	-3.19	0.00	0.1267
$SX5E_{t-1}$	0.0005	0.0002	3.05	0.00	0.1171
R^2	0.5808		LB	$\chi^2(5)$=7.53 [0.184]	
Adj. R^2	0.5509		LM	$\chi^2(5)$=4.26 [0.512]	
N	76		JB	$\chi^2(2)$=209.41 [0.000]	
Std. Error	0.0479		JB/(2)	$\chi^2(2)$=1.05 [0.592]	

Table 5.6: Regression results of the second component of PCA, PCA2. (SX5E Index).

The third principal component of the SX5E index shows almost no autocorrelation and it is has very weak to no correlation with any of the possible independent variables. The highest percentage of variance explained was lower than 15%. Since there is so much room for errors, the third component is not modeled and therefore also not taken into account in the final comparison. For the SX5E index only two principal components will be used.

5.2 Regression models

This section contains the results of the regression models. First five regression models and the Practitioners Black Scholes model are calibrated to the implied volatility surfaces. Afterwards a regression model is chosen, for which time series of the parameters will be constructed. Finally, the modeled implied volatility surfaces can be compared to the historical data.

5.2.1 Calibration

Six regression models are calibrated to the implied volatility surfaces. Table 5.7 and Table 5.8 contain the minimum, maximum and mean of the R squared and adjusted R squared of the regression models of all implied volatility surfaces of the SPX index and the SX5E index. Model 1 (M1) till Model 5 (M5) are described in Section 2.2. The sixth model, the Practitioners Black Scholes model (PBS) is also described in the same section.

Model	R^2			Adjusted R^2		
	Mean	Minimum	Maximum	Mean	Minimum	Maximum
M1	0	0	0	0	0	0
M2	0.741	0.280	0.969	0.732	0.256	0.968
M3	0.902	0.390	0.979	0.895	0.348	0.976
M4	0.918	0.440	0.986	0.912	0.391	0.984
M5	0.924	0.545	0.993	0.917	0.505	0.992
PBS	0.882	0.428	0.971	0.871	0.377	0.969

Table 5.7: This table shows minimum, maximum and mean of the R^2 and adjusted R^2 of the regression models on all implied volatility surfaces of the SPX index.

Model	R^2			Adjusted R^2		
	Mean	Minimum	Maximum	Mean	Minimum	Maximum
M1	0	0	0	0	0	0
M2	0.719	0.332	0.961	0.707	0.303	0.959
M3	0.866	0.356	0.970	0.855	0.297	0.967
M4	0.883	0.386	0.976	0.870	0.314	0.973
M5	0.884	0.382	0.975	0.871	0.310	0.972
PBS	0.842	0.955	0.342	0.825	0.265	0.951

Table 5.8: This table shows minimum, maximum and mean of the R^2 and adjusted R^2 of the regression models on all implied volatility surfaces of the SX5E index.

Model 3, 4 and 5 perform better than the Practitioners Black Scholes model. This indicates that using terms like the logarithm of moneyness instead of moneyness improve the modeling of the implied volatility surfaces. The effects across moneyness are therefore not symmetric, but more asymmetric.

For both the SPX implied volatility surfaces and the SX5E implied volatility surface, Model 4 and 5 give the best results, closely followed by Model 3. Model 3 contains a term for the volatility smile across moneyness, a term for the effects of maturity and a term for the combined effect of maturity and moneyness. Model 4 adds a term that is able to deal with the maturity curvature effect. The addition of the term for the maturity curvature effect only seems to be a marginal improvement. For this reason the time series of the parameters of Model 3, and not Model 4, will be constructed and analyzed. Although Model 5 has a good performance compared to the third model it has two independent variables that have no significant coefficient for more than fifty months and sixty months for the SPX index and SX5E index, respectively. After removing these two terms, the quadratic logarithm of moneyness and the quadratic logarithm of moneyness divided by the square root of maturity, Model 5 has a worse overall performance compared to Model 3. Therefore, only the parameters of Model 3 will be further analyzed.

The maximum number of months that a coefficient is not significant in Model 3 is 20 for the SPX index. For the SX5E index Model 3 has one coefficient which is not significant in 34 months of a total of 78 months.

It is also useful to see where the residuals of the above regression model are the largest. Table A.3 in Appendix A.2 contains the reduction of R squared for each maturity and moneyness of the third regression model for both the SPX index and the SX5E index. It can be seen that the errors are the largest at shorter maturities. For the SX5E index the reduction in R squared is also because of the large error at a maturity of 2 years. The residuals at 80% and 120% moneyness for the SPX index are much higher than residuals at the more near the at-the-money points. For the SX5E index the the errors are not only larger, the higher errors are also more concentrated around the at-the-money points. The third regression model is better at fitting the implied volatilities of near the at-the-money options with longer maturities. The above results are also seen for the other regression models.

5.2.2 Time series of parameters

The parameters of Model 3 for both the SPX index and the SX5E index are shown in Fig. 5.4. The terms that belong to the parameters B1, B2, B3 and B4 are visualized in Fig. A.1 in Appendix A.3. Only for the constant it is clear that it follows the level of the SPX index and the SX5E index, respectively. The correlation coefficient with the VIX index and V2X index is 0.994 and 0.996, respectively. The other parameters are very volatile and therefore probably difficult to model. Table 5.9 shows the correlation coefficients of the coefficients of the third regression model with the VIX/V2X index, returns of the underlying index, realized volatility and the autocorrelation with the first lag of the coefficient themselves. Note that for the SPX index the correlation with the VIX index is shown, while for the SX5E index the correlation with the V2X index is shown.

All time series of the coefficients have quite high autocorrelation. Also, most coefficients have a strong correlation with at least one of the mentioned variables. The most difficult parameters to model, based on this table, are the B2's of both the SPX index and the SX5E index. The B2 parameter belongs to the term moneyness squared divided by maturity.

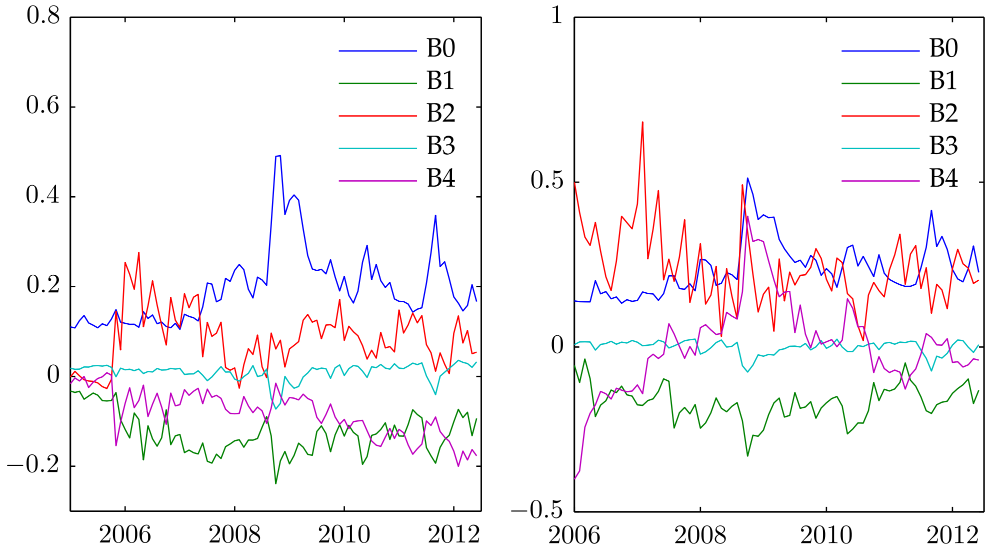

Figure 5.4: The coefficients of regression model 3 for every month for the SPX index (left) and SX5E index (right).

Correlated	Model 3 - SPX				Model 3 - SX5E			
with	B1	B2	B3	B4	B1	B2	B3	B4
VIX/V2X	-0.61	-0.22	-0.78	0.00	-0.66	-0.32	-0.90	0.82
RV	-0.54	-0.21	-0.83	0.11	-0.66	-0.21	-0.89	0.72
Ret	0.34	0.22	0.61	-0.19	0.40	-0.04	0.54	-0.32
1m Lag	0.74	0.64	0.68	0.82	0.66	0.41	0.65	0.92

Table 5.9: This table shows the correlations coefficients between the parameters of model 3 and VIX/V2X index, realized volatility, returns of the underlying index and the one month lag for both the SPX index and the SX5E index.

SPX

The B0 parameter is highly correlated with the VIX index and therefore the VIX index will be used as a regressor. Additional regressors are the one month lag of the B0 parameter and the returns of the SPX index. The regressors are able to explain more than 99% of the variance in parameter B0. The returns of the SPX index have a negative effect on the B0 parameter, which means high returns will lead to a lower implied volatility surface and vice versa. The null hypothesis of both the Ljung-Box test and the Breusch-Pagan can not be rejected, while null hypothesis of the Jarque-Bera test can only not be rejected after the removal of the two largest errors.

Dependent variable: B0 (SPX Index)

Variable	Coefficient	Std. Error	t	p	Part. R^2
C	0.0145	0.0022	6.53	0.00	0.3364
$B0_{t-1}$	0.1602	0.0291	5.51	0.00	0.2653
VIX_t	0.6952	0.0276	25.21	0 .00	0.8832
Ret_t	-0.0684	0.0298	-2.30	0.02	0.0591
R^2	0.9917		LB	$\chi^2(5)$=2.57 [0.776]	
Adj. R^2	0.9914		LM	$\chi^2(3)$=2.19 [0.534]	
N	88		JB	$\chi^2(2)$=71.85 [0.000]	
Std. Error	0.0078		JB/(2)	$\chi^2(2)$=1.17 [0.558]	

Table 5.10: Regression results B0 parameter of the regression model. (SPX Index).

In the regression model of the B1 parameter only the returns of the SPX index and the one month lag of the B1 parameter are used as independent variables. Together they explain almost 65% of the variance in the B1 parameter. The term which the B1 parameter belongs to goes from a negative value to a positive value along moneyness and is zero at 100% moneyness. The absolute value of the term decreases with one over the square root over maturity. The return of the SPX index has a positive effect on the B1 parameter. This means for higher returns the implied volatilities for in-the-money options are decreased, while the implied volatilities for out-of-the-money options are increased. Also the differences across maturity are increased with higher absolute values of the returns of the SPX index. All three null hypotheses (normality of errors, homoskedastic errors and uncorrelated errors) can not be rejected.

The B2 parameter is modeled as an AR(2) model. In the possible AR(1) models with different independent variables the null hypothesis of the Ljung-Box test, the errors terms are uncorrelated, is always rejected. The addition of the two-month lag parameter also increased the variance explained by the regression model. The return of the SPX index is also included as regressor. The term that belongs to the B2 parameter is always positive and decreases with one over maturity. Also, it has a smile across moneyness. The results of the regression models indicate that positive returns of the SPX index would increase the overall level of the implied volatility surface, but especially the implied volatilities at lower maturity. Overall, the model explain more than 45% of the variance in the B2 parameter. The Jarque-Bera test can only not be rejected after the exclusion of the largest error.

The B3 parameter is modeled using an AR(1) model with three additional independent variables, the

Dependent variable: B1 (SPX Index)

Variable	Coefficient	Std. Error	t	p	Part. R^2
C	-0.0377	0.0084	-4.48	0.00	0.1908
$B1_{t-1}$	0.7156	0.0623	11.49	0.00	0.6085
Ret_t	0.2968	0.0592	5.01	0.00	0.2280
R^2	0.6534		LB	$\chi^2(5)$=1.60 [0.902]	
Adj. R^2	0.6452		LM	$\chi^2(2)$=3.47 [0.176]	
N	88		JB	$\chi^2(2)$=1.05 [0.591]	
Std. Error	0.0265		-	-	

Table 5.11: Regression results B1 parameter of the regression model. (SPX Index).

Dependent variable: B2 (SPX Index)

Variable	Coefficient	Std. Error	t	p	Part. R^2
C	0.0251	0.0090	2.78	0.01	0.0849
$B2_{t-1}$	0.4186	0.1017	4.12	0.00	0.1695
$B2_{t-2}$	0.2999	0.1009	2.97	0.00	0.0962
Ret_t	0.2297	0.1064	2.16	0.03	0.0532
R^2	0.4838		LB	$\chi^2(5)$=10.20 [0.070]	
Adj. R^2	0.4652		LM	$\chi^2(3)$=0.78 [0.855]	
N	87		JB	$\chi^2(2)$=11.09 [0.004]	
Std. Error	0.0473		JB/(1)	$\chi^2(2)$=4.43 [0.109]	

Table 5.12: Regression results B2 parameter of the regression model. (SPX Index).

return of the SPX index, the realized volatility of the SPX index and the US AAA corporate bonds excess return. Almost 80% of the variance in the B3 parameter can be explained by the regression model. The error terms are uncorrelated, but there seems to be some heteroskedasticity. After the exclusion of the three largest errors, the null hypothesis of normally distributed error terms can not be rejected. Both the realized volatility and the AAA corporate excess return index have a negative effect on the B3 parameter. The returns of the SPX index however, have a positive effect. The term that belongs to the B3 parameter is the maturity term. This means that a negative B3 parameter would decrease the overall level of the implied volatility surface, but especially the implied volatilities of options with higher maturities.

Dependent variable: B3 (SPX Index)

Variable	Coefficient	Std. Error	t	p	Part. R^2
C	0.2182	0.0944	2.3120	0.0233	0.0605
$B3_{t-1}$	0.2552	0.0878	2.9056	0.0047	0.0923
Ret_t	0.1088	0.0287	3.7864	0.0003	0.1473
RV_t	-0.0884	0.0190	-4.6590	0.0000	0.2073
AAA_t (US)	-0.0019	0.0009	-2.1301	0.0361	0.0518
R^2	0.7906		LB	$\chi^2(5)$=5.53 [0.355]	
Adj. R^2	0.7805		LM	$\chi^2(4)$=10.67 [0.031]	
N	88		JB	$\chi^2(2)$=14.68 [0.001]	
Std. Error	0.0089		JB/(3)	$\chi^2(2)$=2.33 [0.313]	

Table 5.13: Regression results B3 parameter of the regression model. (SPX Index).

The fifth parameter of the regression model, B4, is modeled using three independent variables. The one-month lag of the B4 parameter, the consumer price index level US and the gross domestic product US explain more than 70% of the variance in the B4 parameter. The CPI has a negative impact on the B4 parameter, while the GDP has a positive effect. The term that belongs to the B4 parameter goes from negative to positive across moneyness. It is zero for the at-the-money options and increases with maturity. Both the null hypotheses of the Ljung-Box test and the Breusch-Pagan test can be rejected, while the null hypothesis of the Jarque-Bera test can only be rejected after the exclusion of the largest error.

Dependent variable: B4 (SPX Index)

Variable	Coefficient	Std. Error	t	p	Part. R^2
C	0.2922	0.0884	3.31	0.00	0.1152
$B4_{t-1}$	0.5282	0.0926	5.70	0.00	0.2792
CPI_t (US)	-0.0016	0.0004	-3.70	0.00	0.1398
GDP_t (US)	0.0006	0.0003	1.91	0.06	0.0418
R^2	0.7209		LB	$\chi^2(5)$=4.08 [0.539]	
Adj. R^2	0.7109		LM	$\chi^2(3)$=3.13 [0.372]	
N	88		JB	$\chi^2(2)$=248.17 [0.000]	
Std. Error	0.0268		JB/(1)	$\chi^2(2)$=0.90 [0.636]	

Table 5.14: Regression results B4 parameter of the regression model. (SPX Index).

SX5E

The B0 parameter of the SX5E index, which is highly correlated with the level of the surface is modeled in similar way as the B0 parameter of the SPX index. Both the one month-lag of the B0 parameter and the V2X index are used as regressors. Together they already explain more than 99% of the variance in the B0 parameter. The null hypothesis of uncorrelated errors can not be rejected, just as the null hypothesis of homoskedastic errors.

Dependent variable: B0 (SX5E Index)

Variable	Coefficient	Std. Error	t	p	Part. R^2
C	0.0064	0.0025	2.58	0.01	0.0836
$B0_{t-1}$	0.0648	0.0167	3.89	0.00	0.1716
$V2X_t$	0.8163	0.0145	56.30	0.00	0.9775
R^2	0.9932		LB	$\chi^2(5)$=0.82 [0.976]	
Adj. R^2	0.9930		LM	$\chi^2(2)$=4.36 [0.113]	
N	76		JB	$\chi^2(2)$=0.33 [0.847]	
Std. Error	0.0068		-	-	

Table 5.15: Regression results B0 parameter of the regression model. (SX5E Index).

The B1 parameter is modeled as an AR(1) model with the realized volatility and return of the SX5E index as additional regressors. The model explains more than 60% of the variance in the B1 parameter. The return of the SX5E index has a positive effect on the B1 parameter, which means that in-the-money options will have a decreased implied volatility for higher returns, while the out-of-the-money options will have an increased implied volatility for higher returns. The realized volatility has an opposite effect, meaning the in-the-money options will have an increased implied volatility and the out-of-the-money options will have a decreased implied volatility. Again, the null hypotheses of the three tests can not be rejected.

Dependent variable: B1 (SX5E Index)

Variable	Coefficient	Std. Error	t	p	Part. R^2
C	-0.0547	0.0123	-4.43	0.00	0.2144
$B1_{t-1}$	0.4934	0.0790	6.24	0.00	0.3512
RV_t	-0.1343	0.0384	-3.49	0.00	0.1449
Ret_t	0.1963	0.0746	2.63	0.01	0.0878
R^2	0.6388		LB	$\chi^2(5)$=4.32 [0.504]	
Adj. R^2	0.6237		LM	$\chi^2(3)$=5.77 [0.123]	
N	76		JB	$\chi^2(2)$=4.90 [0.086]	
Std. Error	0.0318		-	-	

Table 5.16: Regression results B1 parameter of the regression model. (SX5E Index).

The B2 parameter is very difficult to model. The highest percentage of variance explained is achieved by the AR(1) model with the indirect real estate total return index of Europe as an additional regressor. Only 30% of the variance in the B2 parameter can be explained. The indirect real estate total return index has a positive effect on the B2 parameter. This means that a high indirect real estate total return index means a larger difference between the implied volatilities of options with different maturities. Options with short maturities will have a larger increase in implied volatility than options with longer maturities, caused by the term that the B2 parameter belongs to. The error of the model seems to be uncorrelated and homoskedastic. After the exclusion of the largest error term, the null hypothesis of normally distrubted errors can not be rejected.

For modeling the B3 parameter, again the US AAA corporate excess return index is used as an independent variable. Together with the V2X index and the realized volatility of the SX5E index, almost 90% of the variance of the B3 parameter can be explained. All independent variables have a negative effect

Dependent variable: B2 (SX5E Index)

Variable	Coefficient	Std. Error	t	p	Part. R^2
C	0.0444	0.0356	1.25	0.22	0.0209
$B2_{t-1}$	0.1650	0.1102	1.50	0.14	0.0298
$INRE_t$ (EU)	0.0004	0.0001	3.94	0.00	0.1754
R^2	0.3114		LB	$\chi^2(5)$=7.19 [0.207]	
Adj. R^2	0.2926		LM	$\chi^2(2)$=2.84 [0.242]	
N	76		JB	$\chi^2(2)$=14.29 [0.001]	
Std. Error	0.0931		JB/(1)	$\chi^2(2)$=5.28 [0.072]	

Table 5.17: Regression results B2 parameter of the regression model. (SX5E Index).

on the B3 parameter. The B3 parameter belongs to the maturity term, this means that if all independent variables are high enough, the B3 parameter will be negative and the level implied volatility surface will be reduced. This is especially the case for higher maturities. There is no autocorrelation between the errors, but there does seem to be some heteroskedasticity. After the exclusion of the largest error, the errors seem to be normally distributed.

Dependent variable: B3 (SX5E Index)

Variable	Coefficient	Std. Error	t	p	Part. R^2
C	0.6157	0.1037	5.93	0.00	0.3285
$V2X_t$	-0.2236	0.0290	-7.71	0.00	0.4525
RV_t	-0.0476	0.0160	-2.97	0.00	0.1090
AAA_t	-0.0054	0.0010	-5.49	0.00	0.2951
R^2	0.8900		LB	$\chi^2(5)$=7.50 [0.186]	
Adj. R^2	0.8854		LM	$\chi^2(3)$=8.64 [0.035]	
N	76		JB	$\chi^2(2)$=83.50 [0.000]	
Std. Error	0.0072		JB/(1)	$\chi^2(2)$=5.37 [0.068]	

Table 5.18: Regression results B3 parameter of the regression model. (SX5E Index).

The B4 parameter is highly correlated with its one-month lag (0.92). The one-month lag of the B4 parameter, with the V2X index and return of the SX5E index, explain more than 90% of the variance in the B4 parameter. The largest proportion of variance is explained by the one-month lag. The V2X index has a positive effect on the B4 parameter, while the return of the SX5E index decreases the B4 parameter if the returns increase. The null hypothesis of the Ljung-Box can not be rejected, but the null hypothesis of the Breusch-Pagan test is rejected. This means that the errors are heteroskedastic. After the exclusion of the largest error term, the null hypothesis of the Jarque-Bera test is not rejected.

Dependent variable: B4 (SX5E Index)

Variable	Coefficient	Std. Error	t	p	Part. R^2
C	-0.0667	0.0230	-2.90	0.00	0.1048
$B4_{t-1}$	0.7238	0.0528	13.72	0.00	0.7233
$V2X_t$	0.2643	0.0869	3.04	0.00	0.1138
Ret_t	-0.3526	0.0963	-3.66	0.00	0.1569
R^2	0.9086		LB	$\chi^2(5)$=7.42 [0.191]	
Adj. R^2	0.9047		LM	$\chi^2(3)$=18.17 [0.000]	
N	76		JB	$\chi^2(2)$=7.63 [0.022]	
Std. Error	0.0407		JB/(1)	$\chi^2(2)$=2.84 [0.242]	

Table 5.19: Regression results B4 parameter of the regression model. (SX5E Index).

5.3 Heston

In this section first the results of the Heston model with jumps (SVJ model) is discussed. Afterwards the calibration of the Heston model will be discussed. From the first unrestricted calibration results, restricted calibrations have been constructed. The results of the unrestricted and restricted calibrations are shown in terms of fit with the implied volatility surface from the historical data. Secondly this section contains the regression models of the calibrated parameters. Finally, the modeled implied volatility surface can be compared to the historical data.

5.3.1 SVJ Model

Before going into a more detailed analysis of the results of the Heston models, it is wise to check whether incorporating jumps is useful or not. The model with jumps has three additional parameters, which are only necessary if a significant decrease in the difference between the modeled implied volatility surface and the implied volatility surface from market data is found. Figure 5.5 shows the mean absolute error of the American implied volatility surfaces computed from the calibrated Heston parameters and the calibrated SVJ (Heston + Jumps) parameters. It can clearly be seen that only in a few cases the mean absolute error is reduced. In most cases the mean absolute error is actually increased. A reason for this to happen is that three additional parameters means a lot more possible local minima in which the calibration procedure could get stuck. Also, the number of data points of each implied volatility surface is quite low, which makes it difficult to calibrate a high number of parameters. Adding jumps to the Heston model is in this case a bad idea and in the remainder of this section only the original Heston model will be analyzed. Analysis of the SVJ model for the SX5E index shows similar results.

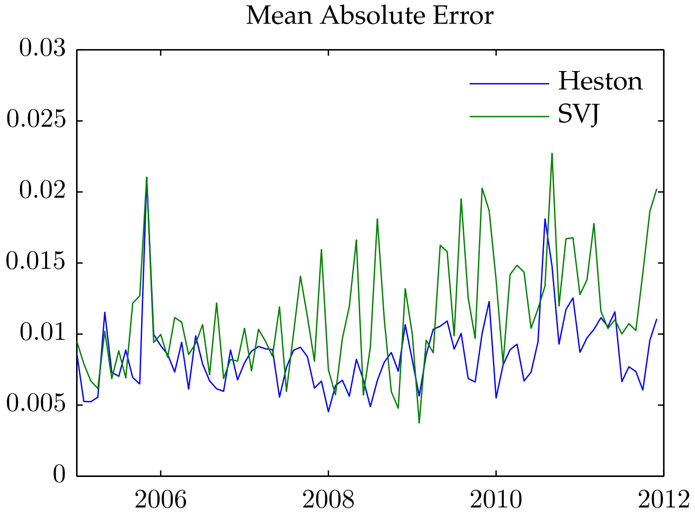

Figure 5.5: The mean absolute error of the calibrated Heston model and SVJ model on market data (SPX index) for every month.

5.3.2 Calibration

Unrestricted parameters

The first calibration of the Heston model was done with almost no restrictions on the parameters. The only restrictions are that the mean reversion rate κ, initial variance V_0, long term variance θ and the volatility of variance η are to be positive and the correlation parameter is to be between -1 and 1. These restrictions are made because the parameters should be interpretable. Figure 5.6 and Fig. 5.7 show the calibrated parameters over time of the SPX and SX5E index, respectively.

For the SPX index, the mean reversion rate, with a mean of 2.81 and standard deviation of 1.70, is quite volatile with some high peaks. The initial variance, with a mean of 0.05 and standard deviation of 0.06, seems to have a similar shape as the mean volatility level over time and therefore also the same shape as the VIX index over time. The correlation coefficient between the initial variance and the VIX index is 0.96 . Since the VIX index is highly correlated with the realized volatility, the initial variance is correlated with the realized volatility as well (0.93). The long term variance shows the same shapes as the initial variance, but with a higher average level. Around the crisis the initial variance is higher than the long term variance. The long term variance is less volatile than the initial variance, and therefore a high correlation is expected with a VIX index from which the high frequency movements are filtered. A Christiano-Fitzgerald filter (Christiano and Fitzgerald (2003)) has been applied to the VIX index, with a minimum frequency of eight months and maximum frequency of infinity. The correlation between the filtered VIX index and the long term variance is 0.91 . The volatility of variance is very volatile and has weak correlation with both the VIX index and realized volatility (0.33 and 0.30). The volatility of variance also has a weak negative correlation with the returns of the underlying SPX index (-0.25). The correlation parameter is negative, which means a positive shock in the spot price is followed by a negative shock in the stochastic volatility. The correlation parameter is negatively correlated with the VIX index (-0.51).

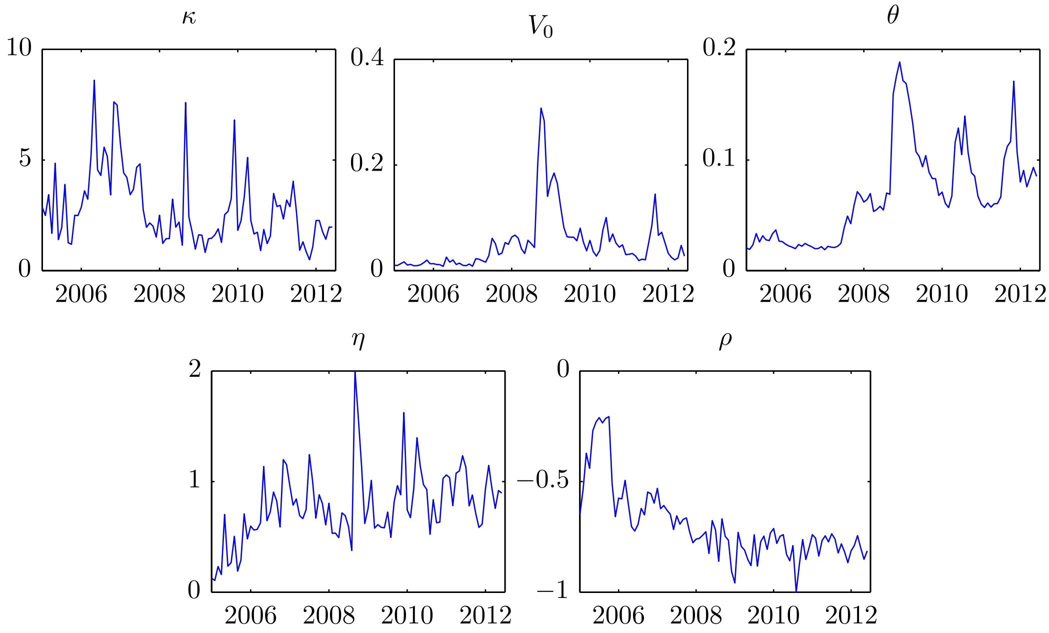

Figure 5.6: The calibrated Heston parameters of the SPX index over time. The top figures contain the mean reversion rate (left), initial variance (middle) and long term variance (right). The bottom figures contain the volatility of variance (left) and correlation coefficient (right).

Since the initial variance has a very high correlation with the VIX index and the long term variance has a very high correlation with the filtered VIX index, the idea is to fix these parameters to these indices using a simple regression. Afterwards the three other parameters, the mean reversion rate, the volatility of variance and the correlation coefficient are calibrated again to try to obtain a better minima.

For the SX5E index, the mean reversion rate is much more volatile and higher than for the SPX index. The mean reversion rate has a mean of 11.04 and standard deviation of 7.67, with peaks of almost 30. The initial variance, with a mean of 0.09 and standard deviation of 0.07, again seems to have a similar

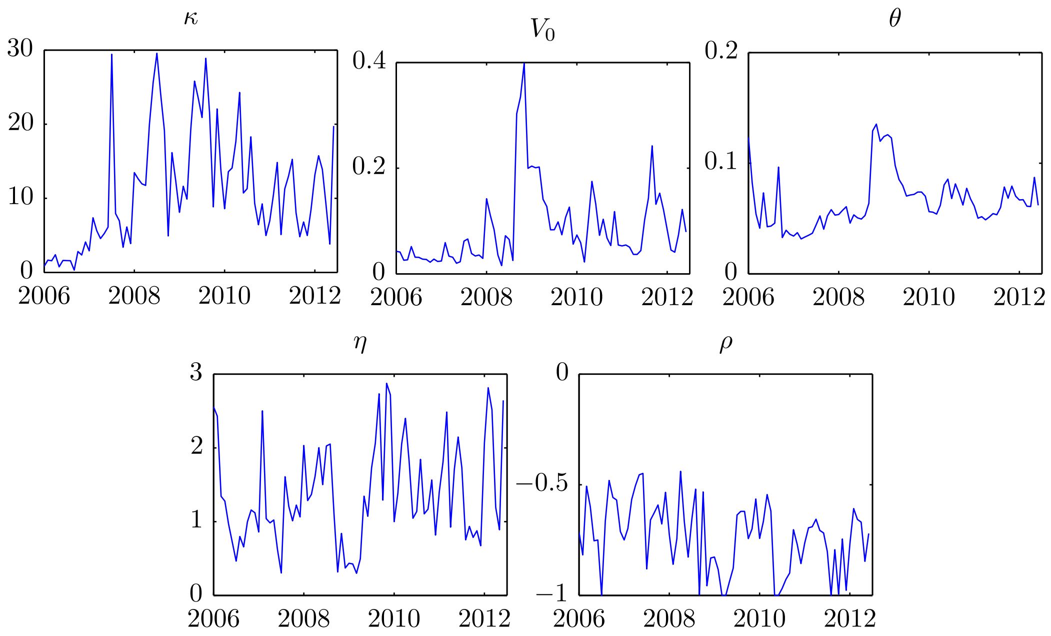

Figure 5.7: The calibrated Heston parameters of the SX5E index over time. The top figures contain the mean reversion rate (left), initial variance (middle) and long term variance (right). The bottom figures contain the volatility of variance (left) and correlation coefficient (right).

shape to the mean volatility level. The correlation coefficient between the initial variance and the V2X index is 0.94 . Since the V2X index is highly correlated with the realized volatility, the initial variance is correlated with the realized volatility as well (0.90).

The long term variance also shows the same shapes as the initial variance, but with a higher average level. Just as for the SPX index, around the crisis the initial variance is higher than the long term variance. For the SX5E index, the long term variance is less correlated with the V2X index (0.75), than the correlation between the long term variance of the SPX index and the VIX index. Also, the correlation with the filtered V2X index is a bit lower (0.73).

The volatility of variance is even more volatile for the SX5E index than for the SPX index. The volatility of variance is also a lot higher for the SX5E index. The volatility of variance does have weak correlations with the V2X index, realized volatility and returns of the underlying (-0.30, -0.30, 0.15). The directions of these correlations are opposite of the same correlations of the volatility of variance of the SPX index. For the SX5E index the correlation coefficient is also negative. The time series is however a lot more volatile compared to the correlation parameter of the SPX index. A standard deviation of 0.20 for the SX5E index compared to a standard deviation of 0.06 for the SPX index. The correlation parameter is negatively correlated with the V2X index (-0.52).

It must be noted that for the SX5E index in five months during the crisis, the lowest minima that was found by the calibration procedure produced really strange results such as a correlation coefficient of +0.7 together with very low mean reversion rate and volatility of variance. An other minima with only a slightly larger calibration error value (3.7E-4 versus 3.3E-4) belonged to parameter which were more in line with the history. For these five months a minima with a slightly larger calibration error has been taken, to obtain parameters which are more in line with the history.

Dependent variable: V_0		Dependent variable: θ	
Indep. Variable	Coefficient	Indep. Variable	Coefficient
Constant	-0.0629	Constant	-0.0303
VIX	0.5258	$\text{VIX}_{\text{Filtered}}$	0.4037
R^2	0.9299	R^2	0.8308

Table 5.20: Simple regression results of the initial variance and long term variance calibrated parameters for the SPX index.

Restricted parameters

Since for the SPX index the initial variance and long term variance are highly correlated with the VIX index and filtered VIX index, respectively, a simple regression is used to restrict these parameters to those respective indices. The results of the simple regression can be seen in Table 5.20. The other three parameters only have the earlier mentioned restrictions to keep them interpretable.

Figure 5.8 shows the results of the newly calibrated mean reversion rate, volatility of variance and correlation coefficient of the SPX index. It can clearly be seen that the parameters that follow from the restricted calibration are even more volatile than the same parameters gotten from the unrestricted calibration. This means that whenever one or two parameters get fixed the other parameters maneuver to very strange values to try and obtain the best fit. It is therefore not a good idea to use these newly obtained time series of the mean reversion rate, volatility of variance and correlation coefficient. In the remainder of this thesis the parameters from the unrestricted calibration will be used.

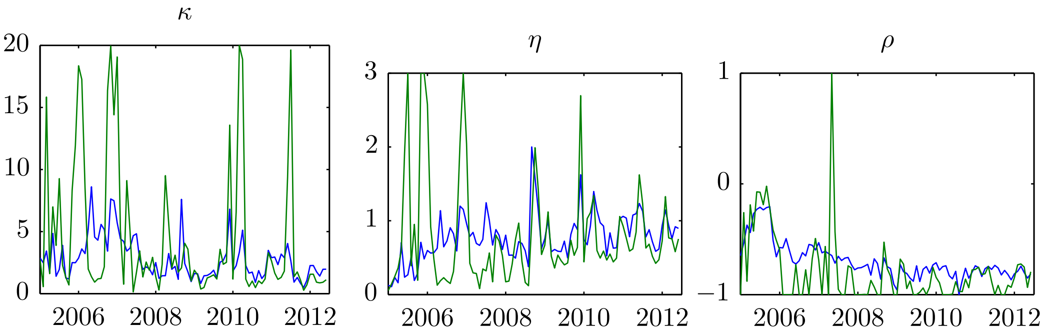

Figure 5.8: The Heston parameters from the restricted calibration and unrestricted calibration of the SPX index over time. The figures contain the mean reversion rate (left), the volatility of variance (middle) and correlation coefficient (right). The blue line indicates the parameter is gotten from an unrestricted calibration, while the green line indicates the parameter is gotten from the restricted calibration.

5.3.3 Time series of parameters

To model all Heston parameters regressions over time have been done. These are mostly AR(1) models, with additional independent variables in the regression. Examples of these additional variables are macroeconomic variables like gross domestic product (GDP) and consumer price index (CPI).

SPX

The mean reversion rate parameter κ of the Heston model should be positive, but when it is modeled over time using a multiple regression model, predicted values are sometimes negative. To overcome this problem, not the mean reversion rate is modeled, but its logarithm. The independent variables that are used are the one-month lag of the logarithm of κ, the nominal US government long term bond (10y) yield, the VIX index and consumer price index US. These variables explain almost 50% of the variance of the logarithm of κ. For all three tests the null hypothesis (uncorrelated errors, homoskedastic errors, normally distributed errors) can not be rejected. The predicted value of the mean reversion rate κ is found by taking the exponent of 'the predicted logarithm of κ plus half of the standard error of the model squared'. Both CPI and NGLR have a positive effect on the logarithm of κ, and therefore also on κ itself. The VIX index has a negative effect on κ. The mean reversion rates is a measure of how quick the volatility goes to the long term variance. A very high mean reversion rate means a flat volatility surface, at all maturities the volatility surface equals the long term variance. The calibrated mean reversion rates show no mean reversion rate higher than 10, therefore the predicted mean reversion rates will be capped at 10.

Dependent variable: log κ (SPX Index)

Variable	Coefficient	Std. Error	t	p	Part. R^2
C	-4.3726	1.8415	-2.37	0.02	0.0636
$\log \kappa_{t-1}$	0.2121	0.1005	2.11	0.04	0.0509
CPI_t (US)	0.0176	0.0074	2.36	0.02	0.0628
NGLR_t (US)	41.9197	9.9221	4.22	0.00	0.1770
VIX_t	-0.9140	0.5186	-1.76	0.08	0.0361
R^2	0.4981		LB	$\chi^2(5)$=1.33 [0.932]	
Adj. R^2	0.4739		LM	$\chi^2(4)$=2.51 [0.643]	
N	88		JB	$\chi^2(2)$=1.19 [0.551]	
Std. Error	0.4218		-	-	

Table 5.21: Regression results logarithm of mean reversion rate parameter of the Heston model κ. (SPX Index).

The initial variance is highly correlated with the level of the implied volatility surface and therefore also the VIX index. For the same reason as the mean reversion rate, the logarithm of the initial variance is modeled instead of the initial variance itself. Another reason is that when the initial variance is modeled the errors tend to be autocorrelated. Almost 95% of the variance in the logarithm of $V0$ can be explained by its one month-lag, the VIX index and the one-month lag of the VIX index. The errors terms are uncorrelated, but there is some heteroskedasticity. After removing the largest error, the null hypothesis of normally distributed errors can not be rejected. The coefficient of the VIX index is positive, but there seems to be some overshooting, making the coefficient of the one-month lag of the VIX index negative. The initial variance is measure of how high or low the short term variance is. The calibrated initial variances show no initial variance lower than 0.015, therefore the predicted initial variances will be floored at 0.01.

Dependent variable: log $V0$ (SPX Index)

Variable	Coefficient	Std. Error	t	p	Part. R^2
C	-1.7166	0.4209	-4.08	0.00	0.1653
$\log V0_t$	0.6628	0.0805	8.23	0.00	0.4464
VIX_t	6.8509	0.4601	14.89	0.00	0.7252
VIX_{t-1}	-4.1372	0.7418	-5.58	0.00	0.2702
R^2	0.9413		LB	$\chi^2(5)$=3.71 [0.591]	
Adj. R^2	0.9392		LM	$\chi^2(3)$=22.78 [0.000]	
N	88		JB	$\chi^2(2)$=36.44 [0.000]	
Std. Error	0.2154		JB/(1)	$\chi^2(2)$=2.78 [0.249]	

Table 5.22: Regression results logarithm of the initial variance parameter of the Heston model $V0$. (SPX Index).

Although the long term variance can not be negative, it is not modeled as a logarithm. The predicted values of the long term variance of both the SPX and SX5E index stay positive. Also the long term variance has a high correlation with the level of the implied volatility surface. The VIX index is therefore included as regressor. Also the one-month lag of the long term variance and the nominal US government long term bond (10y) yield are regressors in this model. More than 90% of the variance in the long term variance parameter can be explained. The largest proportion of variance is explained by the VIX index. The errors are not correlated, but there is some heteroskedasticity. Also, the five largest errors need to be removed before the null hypothesis of normally distributed errors is no longer rejected. The nominal US government long term bond yield has a negative effect on the long term variance, which means the long term variance is decreased when this yield increases. The long term variance is an indication of how high or low the volatility is at higher maturities. The calibrated long term variances show no long term variance higher than 2, therefore the predicted long term variances will be capped at 2.

Dependent variable: θ (SPX Index)

Variable	Coefficient	Std. Error	t	p	Part. R^2
C	0.0306	0.0104	2.93	0.00	0.0929
θ_{t-1}	0.4270	0.0586	7.28	0.00	0.3869
VIX_t	0.1940	0.0188	10.32	0.00	0.5591
NGLR_t (US)	-0.9188	0.2164	-4.25	0.00	0.1767
R^2	0.9301		LB	$\chi^2(5)$=4.09 [0.536]	
Adj. R^2	0.9276		LM	$\chi^2(3)$=12.02 [0.007]	
N	88		JB	$\chi^2(2)$=198.30 [0.000]	
Std. Error	0.0117		JB/(5)	$\chi^2(2)$=4.07 [0.131]	

Table 5.23: Regression results long term variance parameter of the Heston model θ. (SPX Index).

The volatility of variance is the most difficult parameter of the Heston model to predict. For the same reasons as the mean reversion rate, the logarithm of the volatility of variance is modeled instead of the volatility of variance itself. The one-month lag of the logarithm of η, the consumer price index (US) and the nominal US government long term bond (10y) yield explain almost 50% of the variance in the volatility of variance. The errors are uncorrelated and normally distributed, but the errors seem to be heteroskedastic. All regressors have a positive effect on the predicted value of the volatility of variance. The volatility of variance especially influences the shape of the volatility surface at the lower maturities. Based on the calibrated volatility of variances, the predicted volatility of variance is capped at 2.

Dependent variable: $\log \eta$ (SPX Index)

Variable	Coefficient	Std. Error	t	p	Part. R^2
C	-7.4194	1.7416	-4.26	0.00	0.1777
$\log \theta_{t-1}$	0.3766	0.0891	4.23	0.00	0.1755
CPI_t (US)	0.0302	0.0071	4.23	0.00	0.1755
NGLR_t (US)	21.9324	6.9216	3.17	0.00	0.1068
R^2	0.4981		LB	$\chi^2(5)$=3.52 [0.621]	
Adj. R^2	0.4802		LM	$\chi^2(3)$=16.67 [0.001]	
N	88		JB	$\chi^2(2)$=5.72 [0.057]	
Std. Error	0.3514		-	-	

Table 5.24: Regression results logarithm of volatility of variance parameter of the Heston model η. (SPX Index).

The correlation coefficient has the highest correlation with its one-month lag. The one-month lag of the correlation coefficient, together with the consumer price index US is able to account for more than 75% of the variance in the correlation coefficient. The null hypotheses are all rejected, which means the errors are not correlated, are not heteroskedastic and are normally distributed. The correlation coefficient stays between zero and minus one. Sometimes the predicted value is lower than minus one, in these cases the value is set to minus one. A higher consumer price index increases the negative correlation of the volatility and the spot price. A positive correlation means that the volatility will increase with strike price (and therefore moneyness). A negative correlation means that the volatility will decrease with strike price.

Dependent variable: ρ (SPX Index)

Variable	Coefficient	Std. Error	t	p	Part. R^2
C	0.6452	0.2301	2.80	0.01	0.0847
ρ_{t-1}	0.6882	0.0759	9.07	0.00	0.4916
CPI_t (US)	-0.0041	0.0013	-3.25	0.00	0.1105
R^2	0.7767		LB	$\chi^2(5)$=8.89 [0.114]	
Adj. R^2	0.7714		LM	$\chi^2(2)$=4.38 [0.111]	
N	88		JB	$\chi^2(2)$=1.02 [0.600]	
Std. Error	0.0804		-	-	

Table 5.25: Regression results correlation coefficient parameter of the Heston model ρ. (SPX Index).

SX5E

Again the logarithm of the mean reversion rate parameter is modeled. For the SX5E index the one-month lag of the logarithm of the mean reversion rate is used as regressor. In addition the exchange rate of euros to dollars and the indirect real estate total return index of Europe are used. More than 60% of the variance in the logarithm of the mean reversion rate can be explained by the model. The error terms are neither heteroskedastic, nor autocorrelated. After the exclusion of the largest error, the null hypothesis of the Jarque-Bera test can not be rejected. Both a higher indirect real estate index and higher EUR/USD exchange rate will decrease the value of the mean reversion rate. For the SX5E index the predicted mean reversion rate is capped at 30 and floored at 0.3.

Dependent variable: $\log \kappa$ (SX5E Index)

Variable	Coefficient	Std. Error	t	p	Part. R^2
C	5.3359	1.4376	3.71	0.00	0.1606
$\log \kappa_{t-1}$	0.4509	0.1036	4.35	0.00	0.2083
INRE_t (EU)	-0.0020	0.0007	-2.81	0.01	0.0988
EUR/USD_t	-4.6719	1.6231	-2.88	0.01	0.1032
R^2	0.6244		LB	$\chi^2(5)$=8.51 [0.130]	
Adj. R^2	0.6087		LM	$\chi^2(3)$=6.14 [0.105]	
N	76		JB	$\chi^2(2)$=14.70 [0.001]	
Std. Error	0.5671		JB/(1)	$\chi^2(2)$=3.71 [0.157]	

Table 5.26: Regression results logarithm of the mean reversion rate parameter κ of the Heston model. (SX5E Index).

When modeling the initial variance parameter the errors tend to be autocorrelated, however the logarithm of the initial variance parameter does not have this problem and is therefore modeled. The errors of the model of the logarithm of the initial variance parameter are not correlated. The V2X index has the highest correlation with the logarithm of V0, and is therefore used as independent variable. The model explain more than 87% of the variance in the logarithm of the initial variance. The errors are not heteroskedastic and after the exclusion of the two largest errors the null hypothesis of normally distributed errors can not be rejected. The calibrated initial variances show no initial variance lower than 0.015, therefore the predicted initial variances will be floored at 0.01.

The long term variance is modeled using its one-month lag and the V2X index as regressors. The model explains more than 80% of the variance of the long term variance parameter. The V2X index has a positive effect on the long term variance, which makes sense, since both are highly correlated with the overall average level of the implied volatility surface. The null hypothesis of uncorrelated error and homoskedastic errors can not be rejected. After the exclusion of the two largest errors the null hypothesis of normally distributed errors can not be rejected as well. Based on the calibrated volatility of variances, the predicted volatility of variance is capped at 3 and floored at 0.25.

Again the volatility of variance is difficult to model. The logarithm of η is modeled using the V2X index, the one-month lag of the logarithm of the volatility of variance and the EUR/USD exchange rate as

Dependent variable: log V0 (SX5E Index)

Variable	Coefficient	Std. Error	t	p	Part. R^2
C	-4.7217	0.0917	-51.52	0.00	0.9729
$V2X_t$	7.5379	0.3267	23.07	0.00	0.8780
R^2	0.8780		LB	χ^2(5)=10.58 [0.060]	
Adj. R^2	0.8763		LM	χ^2(1)=3.50 [0.061]	
N	76		JB	χ^2(2)=41.67 [0.000]	
Std. Error	0.2653		JB/(2)	χ^2(2)=2.19 [0.334]	

Table 5.27: Regression results logarithm of the initial variance parameter $V0$ of the Heston model. (SX5E Index).

Dependent variable: θ (SX5E Index)

Variable	Coefficient	Std. Error	t	p	Part. R^2
C	-0.0023	0.0039	-0.60	0.55	0.0049
θ_{t-1}	0.4280	0.0575	7.44	0.00	0.4311
$V2X_t$	0.1482	0.0151	9.81	0.00	0.5687
R^2	0.8189		LB	χ^2(5)=4.62 [0.463]	
Adj. R^2	0.8139		LM	χ^2(2)=0.53 [0.765]	
N	76		JB	χ^2(2)=398.19 [0.000]	
Std. Error	0.0103		JB/(2)	χ^2(2)=2.60 [0.273]	

Table 5.28: Regression results long term variance parameter θ of the Heston model. (SX5E Index).

independent variables. The model only explains a bit more than 35% of the variance in the volatility of variance parameter. Both the V2X index and the EUR/USD exchange rate have a negative effect on the volatility of variance. All null hypotheses can not be rejected. The volatility of variance is capped at 3 and floored at 0.25.

Dependent variable: log η (SX5E Index)

Variable	Coefficient	Std. Error	t	p	Part. R^2
C	2.1144	0.8358	2.53	0.01	0.0816
$\log \eta_{t-1}$	0.4004	0.0998	4.01	0.00	0.1828
$V2X_t$	-1.4364	0.5742	-2.50	0.01	0.0800
EUR/US_t	-2.2381	1.1149	-2.01	0.05	0.0530
R^2	0.3685		LB	χ^2(5)=7.21 [0.283]	
Adj. R^2	0.3422		LM	χ^2(3)=3.81 [0.206]	
N	76		JB	χ^2(2)=0.70 [0.702]	
Std. Error	0.4463		-	-	

Table 5.29: Regression results logarithm of the volatility of variance parameter η of the Heston model. (SX5E Index).

The correlation coefficient calibrated from the SX5E index is much more volatile than the correlation coefficient calibrated from the SPX index. It is therefore much more difficult to model. The one-month lag of the correlation coefficient and the V2X index are used as independent variables and only explain 30% of the variance in the correlation coefficient. When the V2X index is high, the correlation coefficient becomes even more negative. There is not autocorrelation in the errors, but there is some heteroskedasticity. After the exclusion of the largest error, the remaining errors are normally distributed.

Since the correlation coefficient can not be lower than minus one, the predicted correlation coefficients is floored at -1. An attempt was made to model the Fisher transformation of the correlation coefficient. The Fisher transformation (Fisher (1915)) maps the real domain $[-1, 1]$ to $[-\infty, \infty]$. Although the mapping would be a good reason to use the Fisher transformation, the Fisher transformation of the correlation coefficient has no high correlations with other variables and only 15% of the variance could be explained.

Dependent variable: ρ (SX5E Index)

Variable	Coefficient	Std. Error	t	p	Part. R^2
C	-0.3999	0.0751	-5.33	0.00	0.2799
ρ_{t-1}	0.1854	0.1074	1.73	0.09	0.0392
$V2X_t$	-0.7475	0.1790	-4.18	0.00	0.1929
R^2	0.3008		LB	$\chi^2(5)$=1.28 [0.937]	
Adj. R^2	0.2816		LM	$\chi^2(2)$=10.27 [0.006]	
N	76		JB	$\chi^2(2)$=11.16 [0.004]	
Std. Error	0.1329		JB/(1)	$\chi^2(2)$=1.81 [0.404]	

Table 5.30: Regression results correlation coefficient ρ of the Heston model. (SX5E Index).

5.4 Benchmark: ORTEC Model

All results are compared to model currently used by ORTEC Finance, explained in Sec. 2.4. An average relative implied volatility surface is used to compute the modeled implied volatility surface from one modeled reference point, the 1 year ATM implied volatility. Figure 5.9 shows the average relative implied volatility surface of the SPX index and the SX5E index. The skew tables are given in Table A.1 and Table A.2, respectively. Both average IV surfaces have a smile across moneyness at the lower maturities. The average IV surface of the SPX index tends to be smoother at longer maturities than the average IV surface of the SX5E index. The latter one has a dent (lower implied volatility) at 100% moneyness, compared to in-the-money and at-the-money implied volatilities.

Overall, the implied volatility tends to be lower for higher moneyness. In the comparison section the calibrations will be compared to the average relative implied volatility surface multiplied with the reference point retrieved from the data (not modeled reference point). Afterwards all modeled implied volatility surface will be compared with the average relative implied volatility surface multiplied with the modeled reference point.

5.4.1 Time series of reference point

The reference point is modeled using a linear regression model with realized volatility, underlying returns and lagged 1 year ATM implied volatility as independent variables. For realized volatility and returns one lagged term is also added. The results for the SPX index and SX5E index are shown in Table 5.31 and Table 5.32, respectively. The model fits quite well, with an adjusted R^2 of 0.96 and 0.92 for the SPX index and SX5E index, respectively. Figure 5.10 shows the regression model fit of the reference points of both implied volatility surfaces.

Dependent variable: 1y ATM Implied Volatility (SPX Index)

Variable	Coefficient	Std. Error	t	p	Part. R^2
C	0.0255	0.0049	5.17	0.00	0.2436
IV_{t-1}	0.7888	0.0316	24.96	0.00	0.8824
RV_t	0.1092	0.0202	5.39	0.00	0.2596
Ret_t	-0.2825	0.0390	-7.24	0.00	0.3873
Ret_{t-1}	0.0680	0.0351	1.94	0.06	0.0432
R^2	0.9635		F(5,83)	437.2 [0.000]	
Adj. R^2	0.9618		LB	$\chi^2(5)$=12.53[0.033]	
N	89		JB	$\chi^2(2)$=1.37 [0.567]	
Std. Error	0.0133		LM	$\chi^2(5)$=22.28 [0.000]	

Table 5.31: Regression results 1y ATM implied volatility (SPX Index).

Lee (2012) states that the coefficients have reasonable interpretation, since positive changes in realized volatility and negative changes in underlying returns result in positive changes in implied volatility.

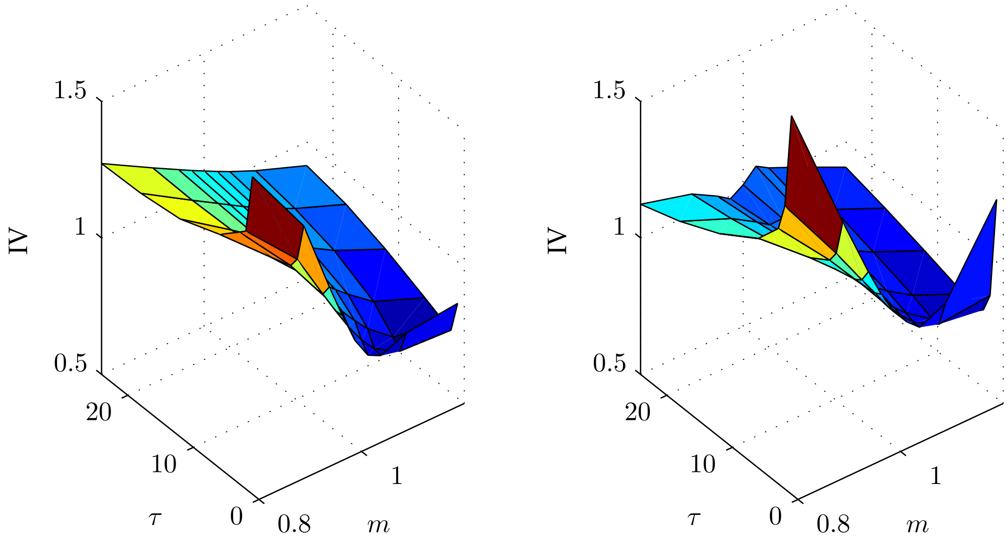

Figure 5.9: The average relative implied volatility surface of the SPX index (left) and the SX5E index (right). The average is taken over the period January 2005 - June 2012.

Dependent variable: 1y ATM Implied Volatility (SX5E Index)

Variable	Coefficient	Std. Error	t	p	Part. R^2
C	0.0364	0.0078	4.64	0.00	0.2326
IV_{t-1}	0.6775	0.0417	16.25	0.00	0.7881
RV_t	0.1749	0.0256	6.83	0.00	0.3968
Ret_t	-0.1325	0.0415	-3.20	0.02	0.1257
Ret_{t-1}	0.0384	0.0393	0.98	0.33	0.0133
R^2	0.9284		F(5,71)	177.2 [0.000]	
Adj. R^2	0.9243		LB	$\chi^2(5)$=10.03[0.126]	
N	77		JB	$\chi^2(2)$=6.89 [0.009]	
Std. Error	0.0167		LM	$\chi^2(5)$=21.43 [0.001]	

Table 5.32: Regression results 1y ATM implied volatility (SX5E Index).

Both models contain significant heteroskedasticity (see Breusch Pagan statistic LM), but Lee (2012) state that the issue does not appear to be severe enough to warrant a more complex model. A possible solution could be to model the reference point in logs rather than levels.

It may seem like the other models have an unfair advantage compared to the benchmark model, since they are modeled using the VIX index. Attempts were made to improve the regression model of the 12 month ATM implied volatility by including the VIX index as independent variable. These attempts all failed, since the R squared of those models were lower than the R squared of the two models given in this section.

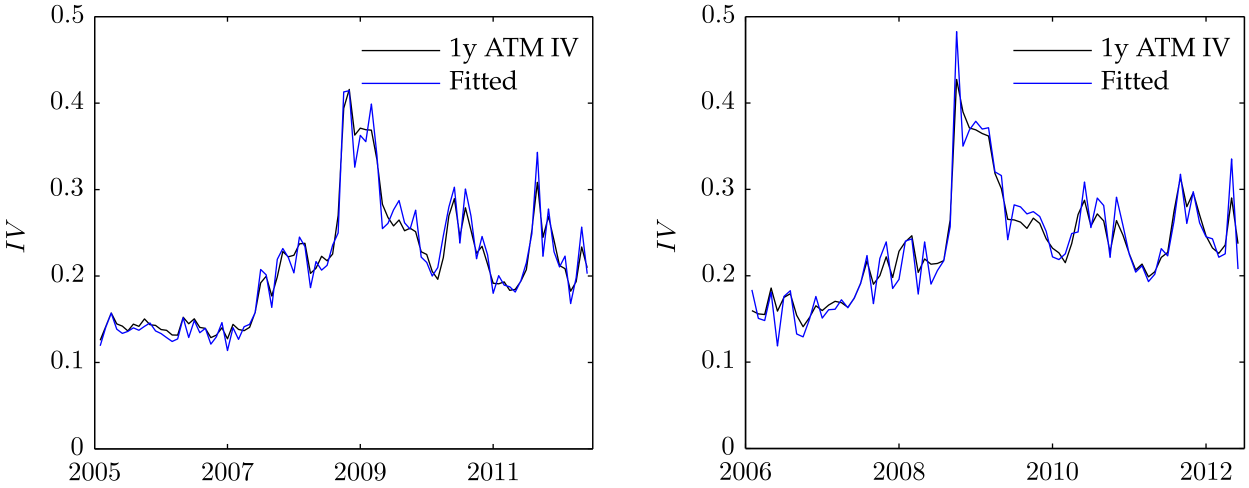

Figure 5.10: The regression model fit of the 1 year ATM implied volatility of the SPX index (left) and the SX5E index (right).

5.5 Comparison

In this section the results of the various models are compared to the historical data, with the current ORTEC model used as a benchmark. The mean absolute error of the modeled implied volatility surfaces will be compared. Since some models do not model the edges of the implied volatility surface very well, the errors in certain segments of the surface will also be compared. A first comparison is done after the calibration step of all four models. Afterwards a comparison is shown between the models with implied volatility surface constructed from parameters/components/reference points modeled over time. All best and worst fits of the four models are shown in Appendix A.4.

5.5.1 After calibration

Figure 5.11 contains the mean absolute error of all (possible) calibrated points of the four models (PCA, Heston, regression, benchmark) with the market data. For both indices (SPX/SX5E) there is room for improvement if the benchmark is compared to the three other models. At this stage, especially PCA seems to be a big improvement over the benchmark model. The Heston model and regression model also look promising, but have a worse performance than PCA for the SX5E index. For the SPX index all three models seem to have the same absolute errors over time. It must be noted that for the SX5E index PCA only models the 90%-110% moneyness implied volatility surface. Errors on the edges (deep in-the-money and deep out-of-the-money) tend to be higher, and therefore it makes sense the PCA calibrations have a smaller mean absolute error than the other models.

Especially around the crisis the benchmark model tends to have a large mean absolute error. For the three other models there is no larger error in the crisis for the SPX index, compared to other times. For the SX5E index the error of the Heston model and regression model does increase during the crisis.

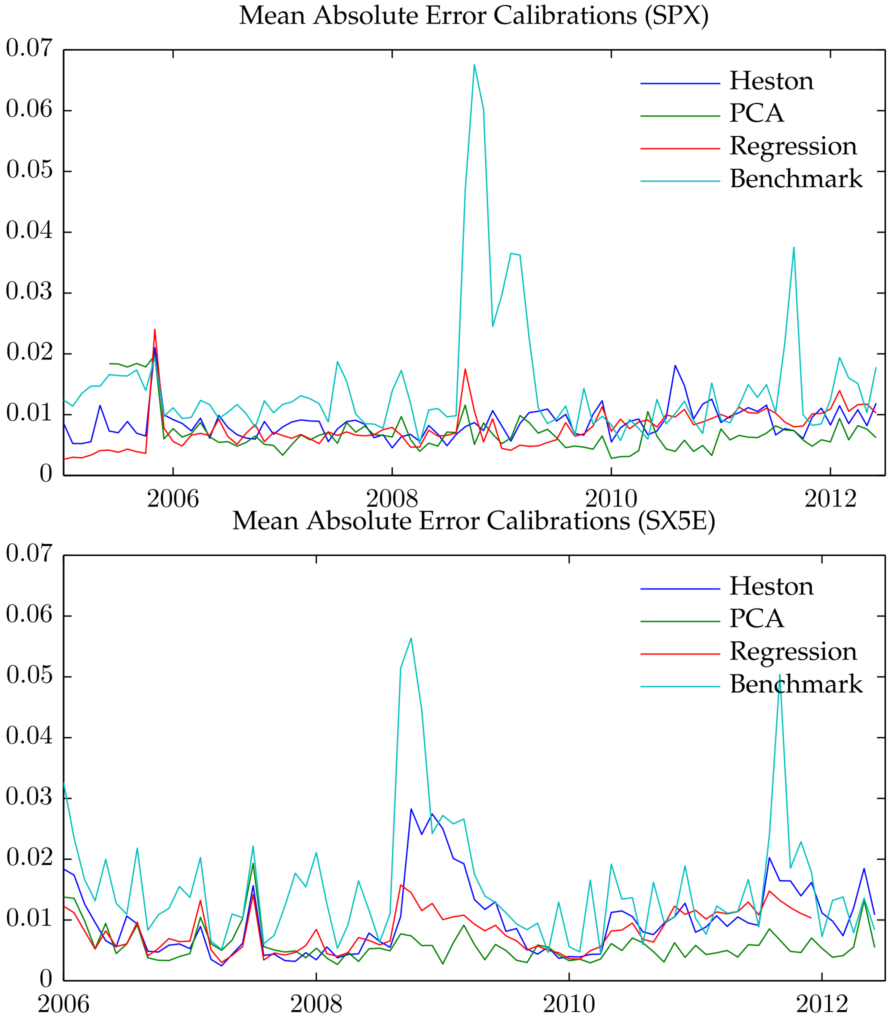
Mean Absolute Error Calibrations (SPX)

Mean Absolute Error Calibrations (SX5E)

Figure 5.11: The mean of the absolute errors of four calibrated models over time of the SPX index and SX5E index. The four models are the Heston model, principal component analysis, regression model and the benchmark model.

5.5.2 Final comparison

The final comparison is made between all four models; PCA, Heston model, regression model and the model of ORTEC (Benchmark). The shapes of the implied volatility surfaces modeled by the first three models are able to change over time, while the relative shape of the model of ORTEC is not. For every month the average absolute error with market data has been calculated over all (possible) modeled points. Figure 5.12 contains this mean absolute error over time for all four models.

It is immediately clear from Fig. 5.12 that the principal component analysis has the largest errors, although they are quite constant over time. The mean absolute error of the principal component analysis has no peaks during for example the crisis, while other models do show a large peak in the mean absolute errors during this time. In the calibration comparison the principal component analysis was the best model, apparently it is very difficult to model the scores of the principal components and therefore the mean absolute error is increased a lot after using the modeled scores of the principal components.

For both indices the regression models has the lowest mean absolute error over time. Although it does not beat the benchmark model every month. Especially during the crisis time the regression model does not show a peak as high as the Heston model and benchmark model. The Heston model seems to have an overall performance which is equal to the benchmark model. During the crisis the peak in the mean absolute error is higher than the mean absolute error of the other models.

Figure 5.14 and Fig. 5.13 show the time-averaged absolute error of each point on the volatility surface. These figures clearly show that all models, but especially the Heston model, have problems with modeling the shorter maturities. At shorter maturities the edges of moneyness (80% / 120%) the averaged absolute error is even larger. The average absolute error surface of the principal component analysis actually looks like a basket, which means that it has difficulty with modeling all edges (short/long maturities and low/high moneyness). These figures also show that the regression model has the smallest absolute errors.

The time and surface averaged absolute error (one value) of every model is given for both the SPX index and the SX5E index in Table 5.33. Since shorter maturities show larger errors an additional averaged absolute error is shown which is averaged over time and the segment of the surface which has a maturity of 3 months or higher. Also, for studies with a short-term horizon sometimes the relative surface of the previous month is used for the benchmark model instead of the averaged relative surface. The time and surface averaged absolute error of this way of modeling the benchmark model is also shown.

The averaged absolute error of PCA for the SPX is, as expected after seeing the figures in this section, much higher than the averaged absolute errors of the other models. For the SX5E index the PCA model shows a similar performance as the benchmark model. It must be noted however that the PCA model for the SX5E index only models 49 points of the implied volatility surface. The Heston model only shows slight improvements over the benchmark model for the SPX index, but much better improvements for the SX5E index. The regression model shows the biggest improvements in terms of minimizing the averaged absolute error in modeling the implied volatility surfaces. Even though excluding the errors of the one-month and two-month maturity points decreases the average absolute error, the same conclusions about the performance of each model compared to the others can still be drawn as when the one-month and two-month maturity points are included.

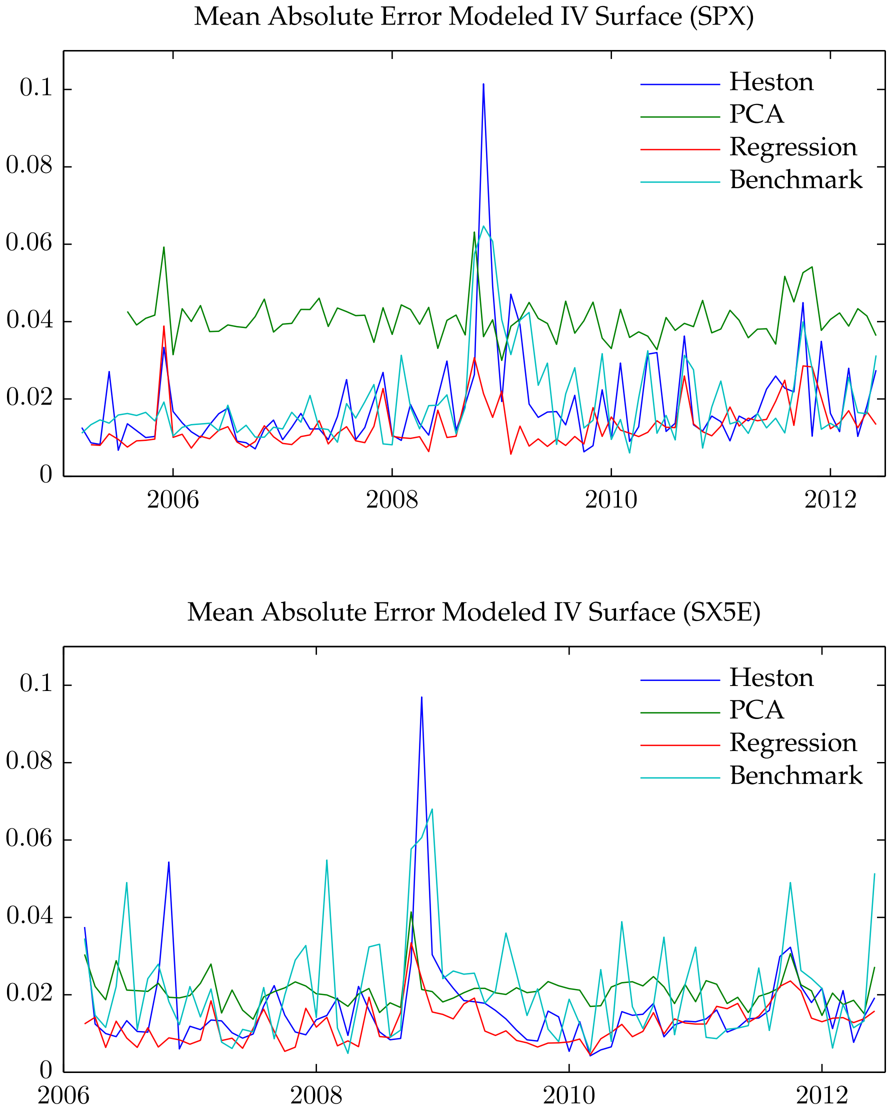

Figure 5.12: The mean of the absolute errors of four modeled IV surfaces of the SPX index and SX5E index over time. The four surfaces are created using the Heston model, principal component analysis, regression model and the benchmark model. The parameters or components of these models are modeled over time.

Mean absolute error per model

Model	SPX All	SPX 3-24m	SX5E All	SX5E 3-24m
Benchmark	0.0192	0.0150	0.0218	0.0188
Benchmark (1mnth)	0.0155	0.0121	0.0210	0.0196
Regression	0.0131	0.0112	0.0123	0.0118
Heston	0.0185	0.0140	0.0164	0.0139
PCA	0.0407	0.0340	0.0210	0.0196

Table 5.33: Mean absolute error per model, averaged over the whole surface. Also the average over a surface, excluding the 1 month and 2 month maturity, are shown.

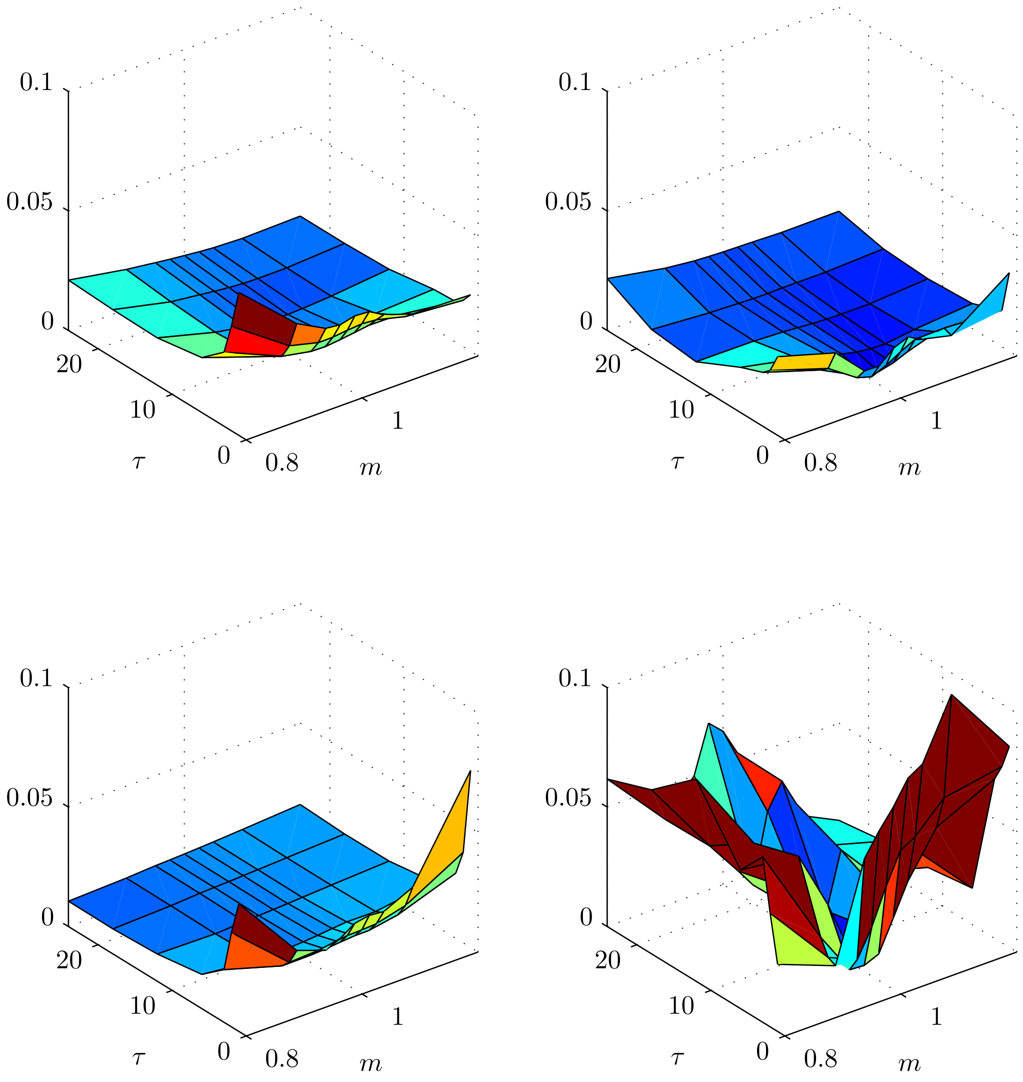

Figure 5.13: Time averaged absolute error for every point of the modeled implied volatility surface of the benchmark model (top left), regression model (top right), Heston model (bottom left) and PCA (bottom right) for the SPX index.

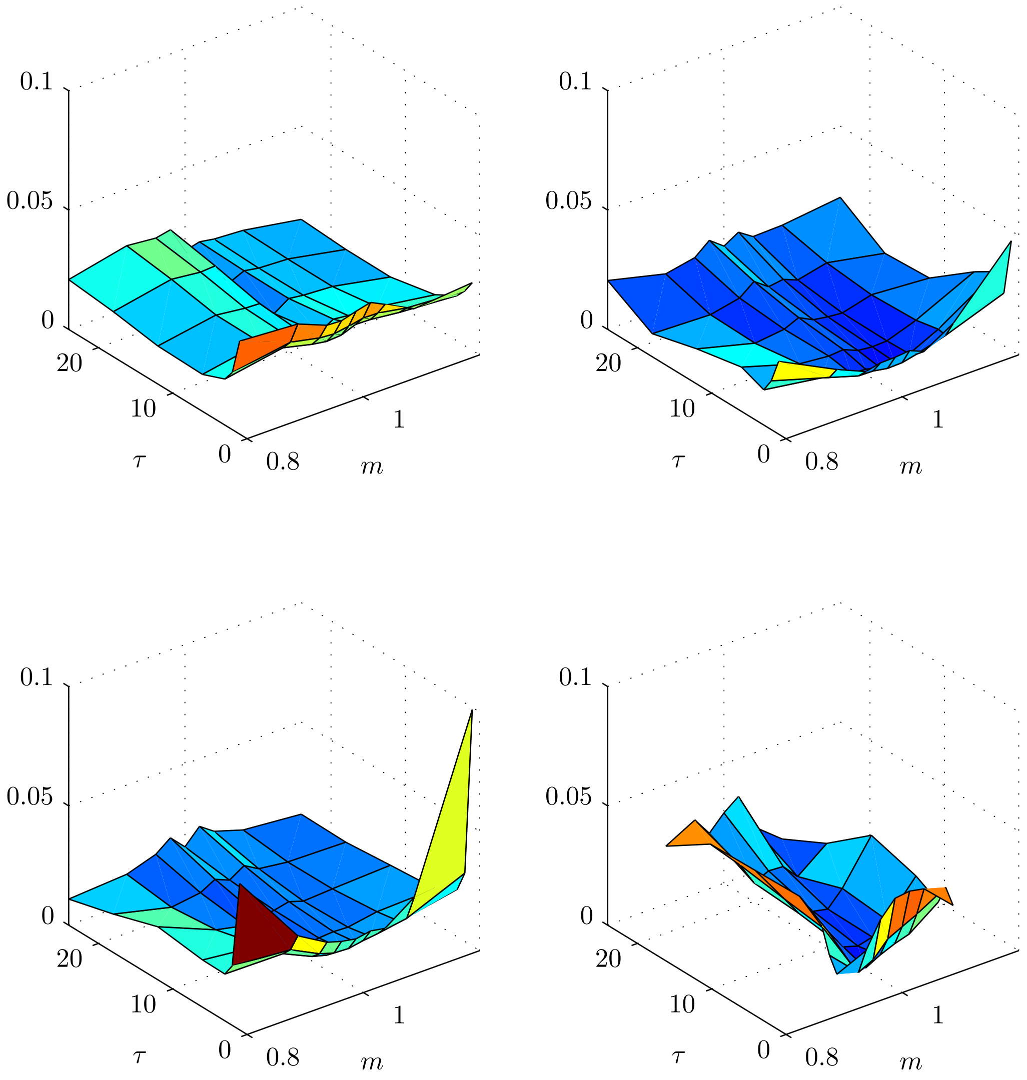

Figure 5.14: Time averaged absolute error for every point of the modeled implied volatility surface of the benchmark model (top left), regression model (top right), Heston model (bottom left) and PCA (bottom right) for the SX5E index.

CHAPTER 6

Conclusion

The conclusion of this thesis consists of conclusions that can be made for the various models and a final conclusion which answers the research question: Does introducing time dependent surface dynamics improve models of the implied volatility surface?

Using principal component analysis more than 99% of the variance in the data can be explained by the first two and three components for the SX5E and SPX index, respectively. The first component has only positive loadings and can be seen as a level factor. The second component varies across maturity (decreasing from a positive value to negative value with higher maturity) and can therefore be seen as a maturity factor. The third component of the SPX index varies mostly across moneyness and can therefore be seen as a moneyness factor.

In the case of this thesis the SVJ model is not an improvement over the Heston model. For the SVJ model three additional parameters need to be calibrated. This probably means that there are a lot more local minima, which makes it difficult to find a better fit of the implied volatility surface. For the SPX index it was tried to restrict two parameters of the Heston model to the VIX index and then recalibrate the other three parameters. This restricted calibration showed worse performance than the unrestricted calibration, because the other three parameters reached very strange and more volatile values trying to find a better fit.

Some parameters of the Heston model are better modeled as logarithms, i.e. the mean reversion rate, initial variance and volatility of variance. The predicted values do need to be capped or floored to not obtain values that are too high or low. An attempt was made to model the Fisher transformation of the correlation coefficient, but did not improve the modeling of this parameter.

After analyzing five different regression models, the third regression model was chosen for further analysis. The terms in the third regression model are a constant, moneyness divided by the square root of maturity, moneyness squared divided by maturity, maturity and moneyness time the square root of maturity. The fourth model was not chosen, since it only showed marginal improvements by adding an additional term. The fifth model also showed better performance in terms of R^2, but had two parameters which are not significant in more than half of the months. Principal component analysis can be used to reduce the number of parameters to a lower amount of component, but the component scores are very difficult to model, so this was not done.

All models had at least one parameter that could be very nicely modeled with the VIX index. This was usually a term that stands for the level of the surface. After calibration of the surfaces a comparison was made between all models. At this stage the PCA showed the best results (lowest mean absolute error), while the regression model and Heston model showed similar performance. All three models showed improvements over the benchmark model, which indicates that there are improvements possible over using a constant surface.

After modeling all parameters over time a final comparison was made between the models. The principal component scores are probably not good enough modeled, because the performance of this model was the worst. It must be noted that the mean absolute error of the PCA model was more or less constant, while other models showed peaks in the mean absolute error during the crisis. The Heston model model showed marginal improvements over the benchmark model for the SPX index, but bigger improvements over the benchmark model for the SX5E index. For both indices the regression model showed the best performance in terms of minimizing the averaged mean absolute error over the whole surface and time. All models show the largest errors in implied volatility at smaller maturities, which are more volatile than implied volatility of longer maturities, and therefore more difficult to model.

Two of three models which are able to model changes in the shape of surface over time show improvements over the benchmark model, which only uses a constant shape. The regression model shows the biggest improvements, reducing the mean absolute error by more than one-third. This means that adding time dependent surface dynamics definitely improves the modeling of the implied volatility surface.

6.1 Recommendations

Recommendations for future research are given below:

- Implicitly a higher weight in calculating errors is given to short maturities, since there are just more market data on short maturities than long maturities. A higher weight can be given to the points that are more relevant. If one wants a better performance at longer maturities, higher weights could be given to these points. In some literature, e.g. Moodley (2005), the spread in bid-ask prices is used as a weight. Hamida and Cont (2005) suggest to use the implied volatility as weights.
- The local minima of the Heston model are a huge problem in the calibration procedure. Using a simple minimizer from a lot of different starting positions is not really an efficient way to find the best or one of the best minima. Differential Evolution, by Storn and Price (1997), is a promising minimizer which might work better than the previously mentioned method. Even after finding a local minimum it will keep searching for a given amount of time to even better minimum. If this minimizer works better, the SVJ model could be given another shot.
- Christoffersen and Jacobs (2004) state that when comparing models, the same loss functions should be used in the estimation stage. In this thesis the loss function in obtaining the parameters of the Heston model is based on prices, while for other models the loss function is based on implied volatilities. In future research the performance of the Heston model with a loss function based on implied volatilities should be compared with the performance of the Heston model with a loss function based on prices.
- Two models used in this thesis to describe the implied volatility surface are principal component analysis and a regression model. Park et al. (2009) modeled time series with semi parametric factor dynamics. The model they used is similar to principal component analysis, but uses an unobserved nonparametric function of independent variables instead of a linear combination of independent variables. A simple form of the equation is:

  $$Y_{t,j} = Z_t^T m(X_{t,j}) + \varepsilon_{t,j}, \tag{6.1}$$

  where $Y_{t,j}$ is the dependent variable, Z is an unobserved L-dimensional process, $m()$ are unknown real-valued functions of the independent variables $X_{t,j}$. Before estimation, one should determine the number of dynamic functions (also the dimension of Z). Park et al. (2009) applied the above model on intraday implied volatilities based on the German stock index DAX (ODAX) prices. Afterwards the time series of the estimated component scores/parameters $\hat{Z}_{t,k}$ $(k \leq J)$ can be modeled over time in similar fashion as the component score of principal component analysis.
- In a few years, when there is more data available, it would be a good idea to test the actual performance (out of sample) of these models!
- The next step after modeling a better implied volatility surface, would be to model a better volatility cube. A volatility cube contains the implied volatilities of swaptions. The term cube comes from the three-dimensional aspect of swaptions. Options have only two dimensions (moneyness and maturity), while swaptions have three dimensions (moneyness, tenor of the underlying swap and maturity of the option), Trolle and Schwartz (2010). For the volatility cube there is no nice

model such as the Heston model, but since the regression model worked very well for the volatility surface, it could also work for the volatility cube. First one would have to identify stylized facts or trends and afterwards try to incorporate them into terms of moneyness, tenor and maturity. Principal component analysis could also work, although it will be difficult to find data for all necessary points of the volatility cube.

Acknowledgements

First I would like to thank the people at ORTEC Finance for letting me do this thesis at their company, Bert Kramer for allowing me to do this thesis at the research department, Paul and Ingmar of EFIS for the healthy food tips during lunches, all colleagues at the P&I department for half a year of fun work and of course Kai Ming Lee for being my supervisor at ORTEC Finance. If I got stuck, a few discussions with him allowed me to continue working and writing on my thesis.

Secondly, I would like to thank professor Dick van Dijk for being my supervisor at the Erasmus University. Although we did not have many meetings, the feedback was very useful in terms of improving my thesis. Also I would like to thank Michel van der Wel for co reading my thesis and also giving feedback on the final concept.

Finally, I would like to thank Annette, for her continuous support during my studies.

Bibliography

S. Aboura. Pricing CAC 40 index options with stochastic volatility. 2003.

K. Ahoniemi. Modeling and forecasting the VIX index. 2008.

H. Albrecher, P. Mayer, W. Schoutens, and J. Tistaert. The little Heston trap. 6(05), 2006.

A. Alentorn. Modelling the implied volatility surface: an empirical study for ftse options. Working paper. University of Essex, UK., 2004.

I.U. Badshah. Modelling the dynamics of implied volatility surfaces. Working paper. Available at: http://ssrn.com/abstract=1347981, 2009.

D.S. Bates. Jumps and stochastic volatility: Exchange rate processes implicit in deutsche mark options. *The Review of Financial Studies*, 9:69–107, 1996.

S. Beckers. Standard deviations implied in option prices as predictors of future stock price variability. *Journal of Banking and Finance*, 5:363–381, 1981.

C. Bin. Calibration of the heston model with application in derivative pricing and hedging. *Master's thesis, Department of Mathematics, Technical University of Delft, Delft, The Netherlands*, 2007.

F. Black and M. Scholes. The pricing of options and corporate liabilities. *The Journal of Political Economy*, 81:637–654, 1973.

J.P. Boyd. *Chebyshev and Fourier spectral methods*. Dover Pubns, 2001.

T.S. Breusch and A.R. Pagan. A simple test for heteroscedasticity and random coefficient variation. *Econometrica: Journal of the Econometric Society*, pages 1287–1294, 1979.

D. Brigo and F. Mercurio. Lognormal-mixture dynamics and calibration to market volatility smiles. *International Journal of Theoretical and Applied Finance*, 5(4):427–446, 2002.

L. Canin and S. Figlewski. The information content of implied volatility. *The Review of Financial Studies*, 6:659–681, 1993.

P. Carr and D. Madan. Option valuation using the fast fourier transform. *Journal of Computational Finance*, 2(4):61–73, 1999.

D.P. Chiras and S. Manaster. The information content of option prices and a test of market efficiency. *Journal of Financial Economics*, 6:213–234, 1978.

B.J. Christensen and N.R. Prabhala. The relation between implied and realized volatility. *Journal of Financial Economics*, 50:125–150, 1998.

L.J. Christiano and T.J. Fitzgerald. The band pass filter. *International Economic Review*, 44:435–465, 2003.

P. Christoffersen and K. Jacobs. The importance of the loss function in option valuation. *Journal of Financial Economics*, 72(2):291–318, 2004.

J.C. Cox and S.A. Ross. The valuation of options for alternative stochastic processes. *Journal of financial economics*, 3(1):145–166, 1976.

T.E. Day and C.M. Lewis. Stock market volatility and the information content of stock index options. *Journal of Econometrics*, 5:267–287, 1992.

B. Dumas, J. Fleming, and R.E. Whaley. Implied volatility functions: Empirical tests. *The Journal of Finance*, 53(6):2059–2106, 1998.

C.B.O. Exchange. Vix white paper. *URL: http://www. cboe. com/micro/vix/vixwhite. pdf*, 2003.

F. Fang and C.W. Oosterlee. A novel pricing method for european options based on fourier-cosine series expansions. *SIAM Journal on Scientific Computing*, 31:826–843, 2008.

G. Fiorentini, A. Leon, and G. Rubio. Estimation and empirical performance of heston's stochastic volatility model: the case of a thinly traded market. *Journal of Empirical Finance*, 9(2):225–255, 2002.

R.A. Fisher. Frequency distribution of the values of the correlation coefficient in samples from an indefinitely large population. *Biometrika*, 10(4):507–521, 1915.

J. Gatheral. Modeling the implied volatility surface. *Global Derivatives and Risk Management, Barcelona*, 2003.

J. Gatheral. *The volatility surface: a practitioner's guide*, volume 357. Wiley, 2006.

P. Giot. The information concent of implied volatility in agricultural commodity markets. *The Journal of Futures Markets*, 23:441–454, 2003.

D. Guo. The risk premium of volatility implicit in currency options. In *Computational Intelligence for Financial Engineering (CIFEr), 1998. Proceedings of the IEEE/IAFE/INFORMS 1998 Conference on*, pages 224–251. IEEE, 1998.

S.B. Hamida and R. Cont. Recovering volatility from option prices by evolutionary optimization. *Journal of Computational Finance*, 8(4):43–76, 2005.

S.L. Heston. A closed-form soluiton for options with stoachastic volatility with applications to bond and currency options. *The Review of Financial Studies*, 6:327–343, 1993.

J.C. Hull. *Options, Futures and other Derivatives*. Pearson Education Limited, eight edition, 2012.

C.M. Jarque and A.K. Bera. A test for normality of observations and regression residuals. *International Statistical Review/Revue Internationale de Statistique*, pages 163–172, 1987.

I.T. Jolliffe. *Principal component analysis*, volume 2. Wiley Online Library, 2002.

P. Jorion. Predicting volatility in the foreign exchange market. *The Journal of Finance*, 50:507–528, 1995.

M. Kamal and J. Gatheral. Implied volatility surface. *Encyclopedia of Quantitative Finance*, 2010.

C.G. Lamoureux and W.D. Lastrapes. Forecasting stock-return variance: Toward an understanding of stochastic implied volatilities. *The Review of Financial Studies*, 6:293–326, 1993.

K.M. Lee. Internal memo, equity implied volatility and swaption interest implied volatility. 2012.

R.W. Lee. Implied volatility: Statics, dynamics, and probabilistic interpretation. Technical report, Standford University, 2002. Forthcoming in *Recent Advances in Applied Probability*.

Y.N. Lin, N. Strong, and X. Xu. Pricing ftse 100 index options under stochastic volatility. *Journal of futures Markets*, 21(3):197–211, 2001.

G.M. Ljung and G.E.P. Box. On a measure of lack of fit in time series models. *Biometrika*, 65(2):297–303, 1978.

Matlab. URL `http://www.mathworks.se/help/toolbox/optim/ug/fmincon.html`.

A. Matytsin. Modeling volatility and volatility derivatives. In *Columbia Practitioners Conference on the Mathematics of Finance*, 1999.

R.C. Merton. Theory of rational option pricing. *The Bell Journal of Economics and Management Science*, 4: 141–183, 1973.

N. Moodley. The heston model: A practical approach. *University of the Witwatersand Paper*, 2005.

E. Nilsson. *Calibration of the Volatility Surface.* Masters Thesis, Royal Insititute of Technology, Stockholm, 2008.

B. U. Park, E. Mammen, W. Härdle, and S. Borak. Time series modelling with semiparametric factor dynamics. *Journal of the American Statistical Association*, 104(485):284–298, 2009.

I. Peña, G. Rubio, and G. Serna. Why do we smile? on the determinants of the implied volatility function. *Journal of Banking & Finance*, 23:1151–1179, 1999.

K. Pearson. Liii. on lines and planes of closest fit to systems of points in space. *The London, Edinburgh, and Dublin Philosophical Magazine and Journal of Science*, 2(11):559–572, 1901.

R. le Roux. A long-term model of the dynamics of the s&p 500 implied volatility surface. *North American Actuarial Journal*, 11:61–75, 2007.

D.P. Simon. The nasdaq volatility index during and after the bubble. *The Journal of Derivatives*, 11(2): 9–24, 2003.

R. Storn and K. Price. Differential evolution–a simple and efficient heuristic for global optimization over continuous spaces. *Journal of global optimization*, 11(4):341–359, 1997.

A. Trolle and E.S. Schwartz. The swaption cube. 2010.

P. Wilmott. *Paul Wilmott introduces quantitative finance.* Wiley, 2007.

APPENDIX A

Appendix

A.1 Average Skew IV Surface

$\tau \setminus m$	80%	90%	95%	97.5%	100%	102.5%	105%	110%	120 %
1M	1.66	1.40	1.13	1.00	0.89	0.81	0.79	0.83	0.85
2M	1.45	1.25	1.08	1.00	0.92	0.85	0.80	0.74	0.73
3M	1.42	1.21	1.08	1.01	0.96	0.90	0.85	0.77	0.74
6M	1.36	1.19	1.09	1.05	1	0.96	0.92	0.85	0.77
12M	1.30	1.17	1.10	1.07	1.04	1.00	0.97	0.92	0.84
18M	1.28	1.65	1.11	1.08	1.05	1.03	1.00	0.96	0.89
24M	1.27	1.69	1.12	1.09	1.07	1.05	1.02	0.98	0.91

Table A.1: Average implied volatility (Jan 2005 - Dec 2011) relative to the 1 year ATM implied volatility of the SPX index.

$\tau \setminus m$	80%	90%	95%	97.5%	100%	102.5%	105%	110%	120 %
1M	1.89	1.41	1.18	1.08	0.99	0.94	0.89	0.94	1.23
2M	1.54	1.28	1.13	1.07	0.99	0.94	0.89	0.84	0.86
3M	1.43	1.23	1.12	1.06	1.00	0.95	0.91	0.84	0.79
6M	1.34	1.18	1.09	1.05	1	0.97	0.93	0.87	0.79
12M	1.24	1.13	1.07	1.03	1.00	0.99	0.96	0.91	0.83
18M	1.18	1.09	1.04	1.01	1.01	1.03	1.00	0.96	0.87
24M	1.12	1.07	1.02	0.99	1.02	1.07	1.04	1.00	0.91

Table A.2: Average implied volatility (Jan 2006 - Dec 2011) relative to the 1 year ATM implied volatility of the SX5E index.

A.2 Regression Model 3: Reduction in R squared

This appendix contains a table with the maximum, minimum and mean reduction in R^2 of Regression model 3 over different maturities and moneyness. The results of the other regression models are more or less the same, not in magnitude, but in the sense that short maturities contribute more to the reduction in R^2, than long maturities. Also for all models the 80% moneyness and 120% show the largest errors.

	SPX			SX5E		
τ	Mean	Maximum	Minimum	Mean	Maximum	Minimum
1	0.0457	0.4077	0.0070	0.0396	0.2681	0.0060
2	0.0173	0.1055	0.0025	0.0107	0.1107	0.0012
3	0.0117	0.0621	0.0016	0.0121	0.1386	0.0018
6	0.0114	0.0406	0.0014	0.0162	0.0711	0.0017
12	0.0049	0.0188	0.0002	0.0120	0.0489	0.0006
18	0.0009	0.0042	0.0000	0.0116	0.0624	0.0007
24	0.0052	0.0174	0.0000	0.0295	0.1402	0.0013
m						
0.8	0.0201	0.0766	0.0017	0.0117	0.0566	0.0031
0.9	0.0161	0.0392	0.0018	0.0132	0.0429	0.0021
0.95	0.0061	0.0484	0.0014	0.0126	0.0371	0.0042
0.975	0.0051	0.0647	0.0003	0.0223	0.0791	0.0030
1.0	0.0072	0.0804	0.0001	0.0144	0.1372	0.0005
1.025	0.0095	0.0941	0.0003	0.0246	0.2879	0.0019
1.05	0.0095	0.1021	0.0008	0.0124	0.0726	0.0023
1.1	0.0097	0.1026	0.0003	0.0195	0.0830	0.0044
1.2	0.0138	0.0823	0.0010	0.0354	0.0584	0.0140

Table A.3: This table shows mean, maximum and minimum reduction of the R^2 the third regression model over different maturities and moneyness for the SPX and the SX5E index.

A.3 Terms of Regression Model 3

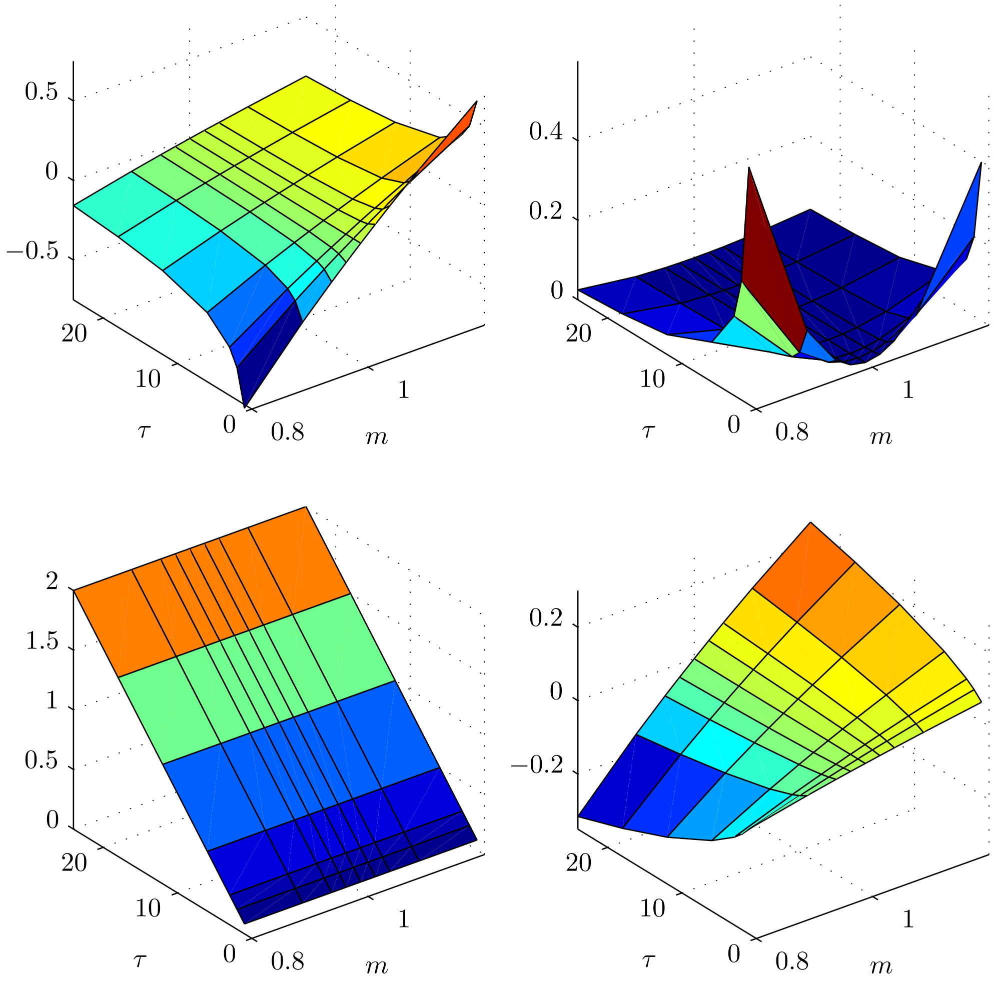

Figure A.1: The four terms that belong to the B1 (top left), B2 (top right), B3 (bottom left) and B4 (bottom right) coefficient of regression model three.

A.4 Worst and best fits

A.4.1 SPX

Benchmark

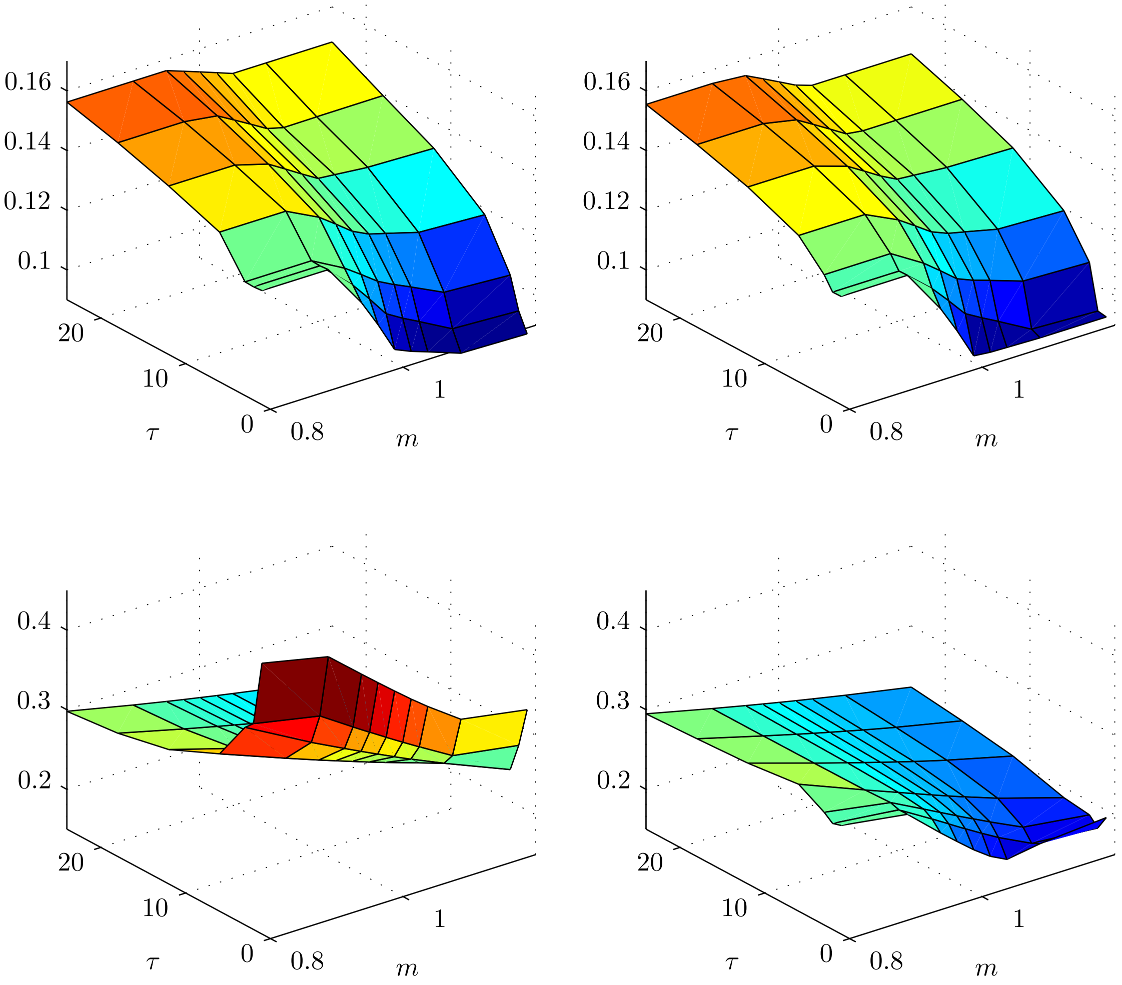

Figure A.2: The implied volatility surface from historical data (left) and the modeled (Benchmark) implied volatility surface (right) of the SPX index, at July 2005 (top) and September 2008 (bottom). July 2005 has the best fit, while September 2008 has the worst fit.

Heston

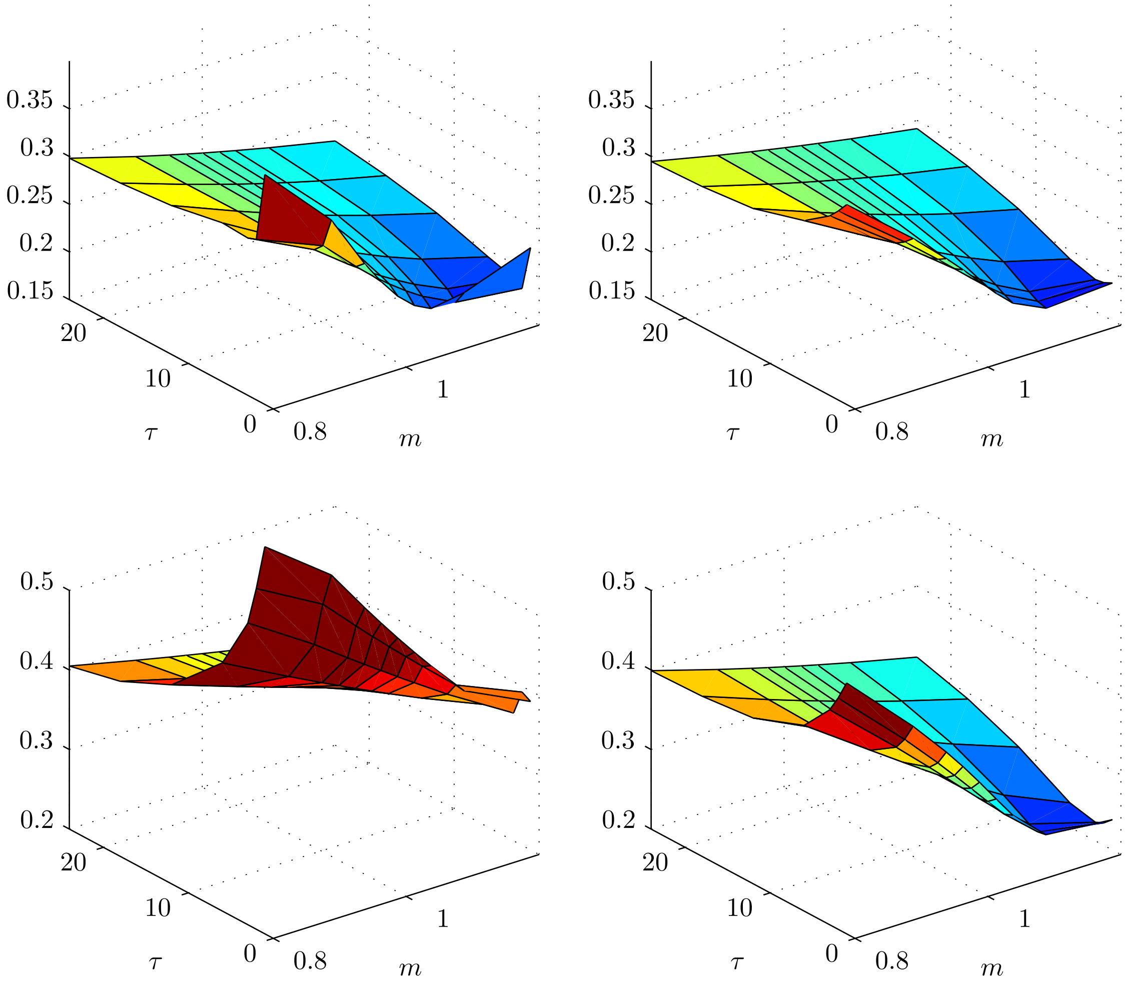

Figure A.3: The implied volatility surface from historical data (left) and the modeled (Heston) implied volatility surface (right) of the SPX index, at September 2009 (top) and November 2008 (bottom). September 2009 has the best fit, while November 2008 has the worst fit.

PCA

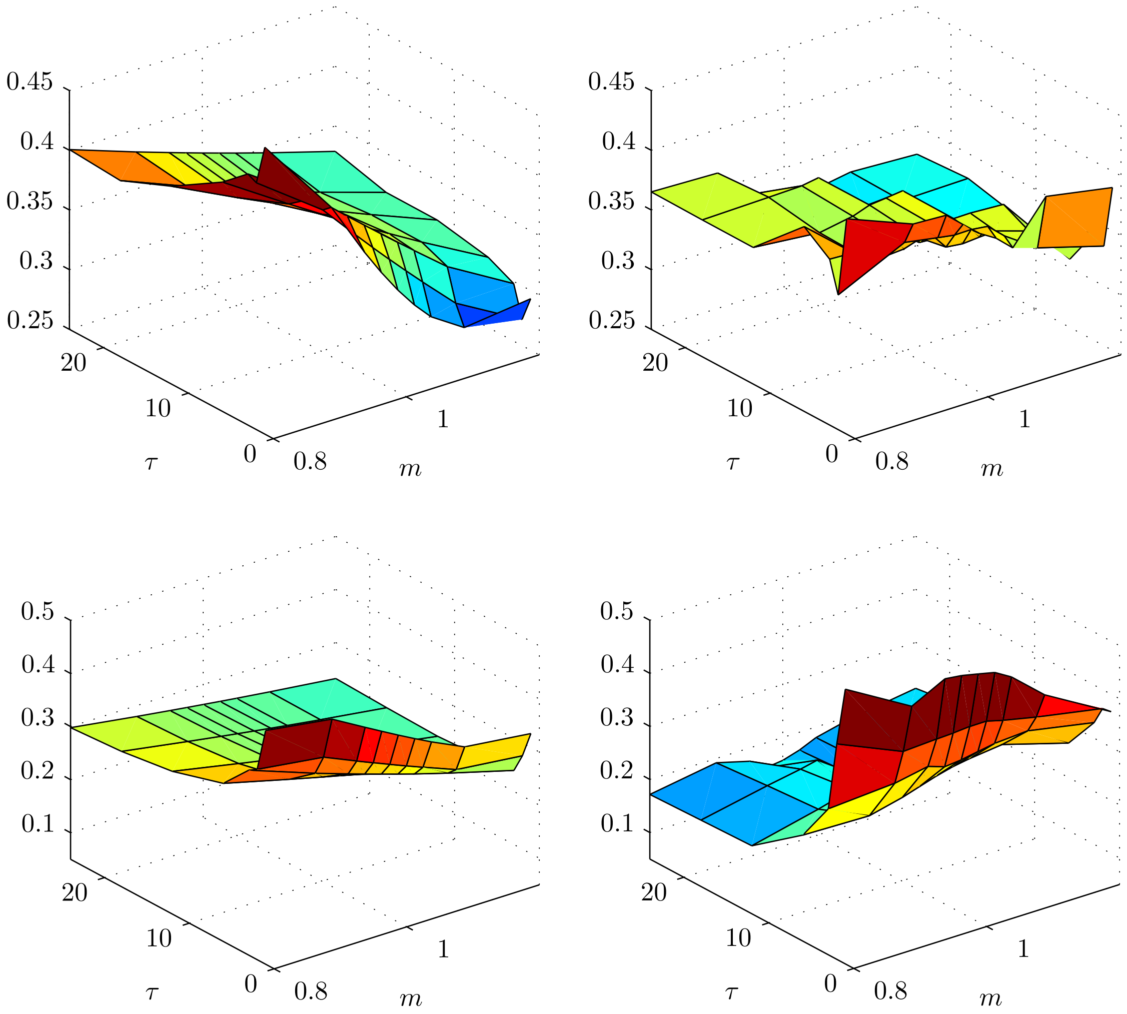

Figure A.4: The implied volatility surface from historical data (left) and the modeled (PCA) implied volatility surface (right) of the SPX index, at December 2008 (top) and September 2008 (bottom). December 2008 has the best fit, while September 2008 has the worst fit.

Regression

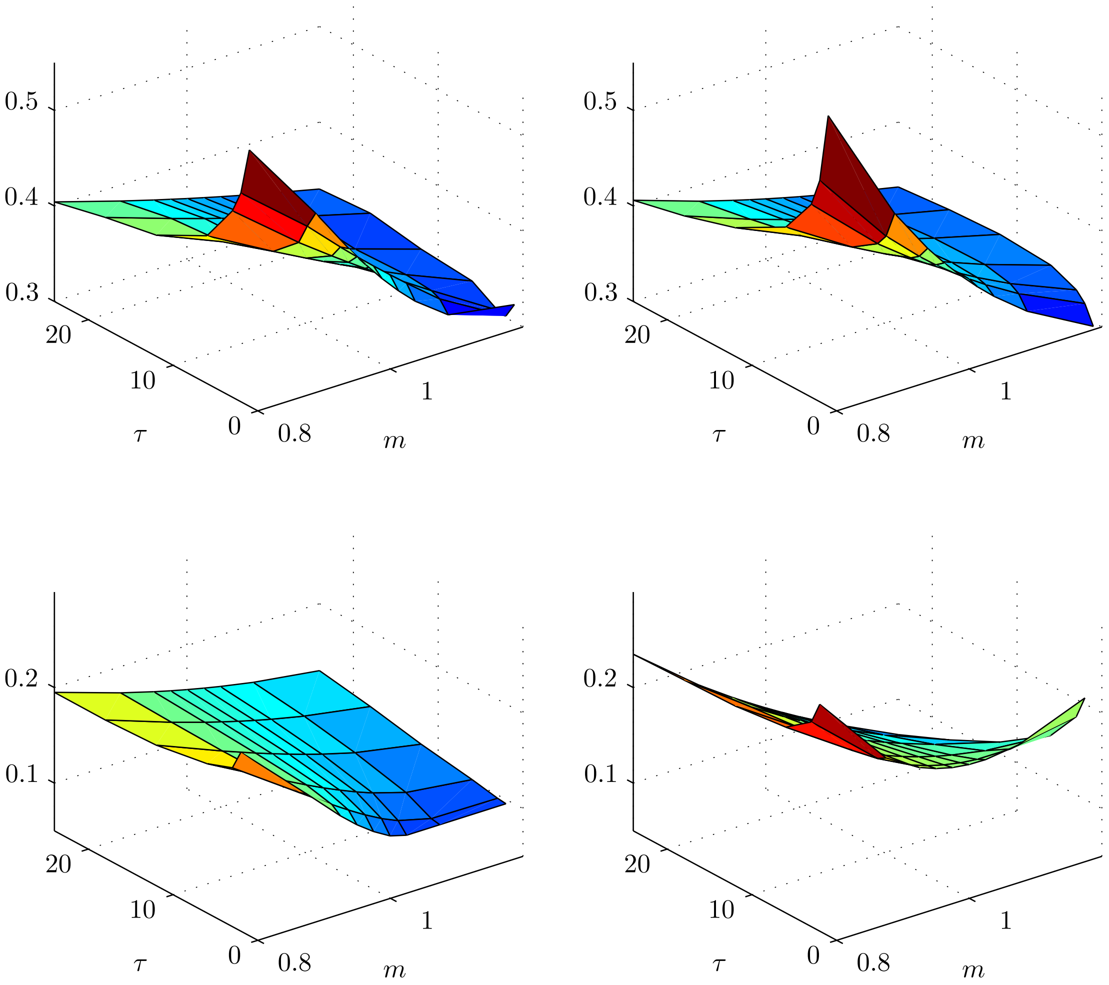

Figure A.5: The implied volatility surface from historical data (left) and the modeled (Regression) implied volatility surface (right) of the SPX index, at January 2009 (top) and November 2005 (bottom). January 2009 has the best fit, while November 2005 has the worst fit.

A.4.2 SX5E

Benchmark

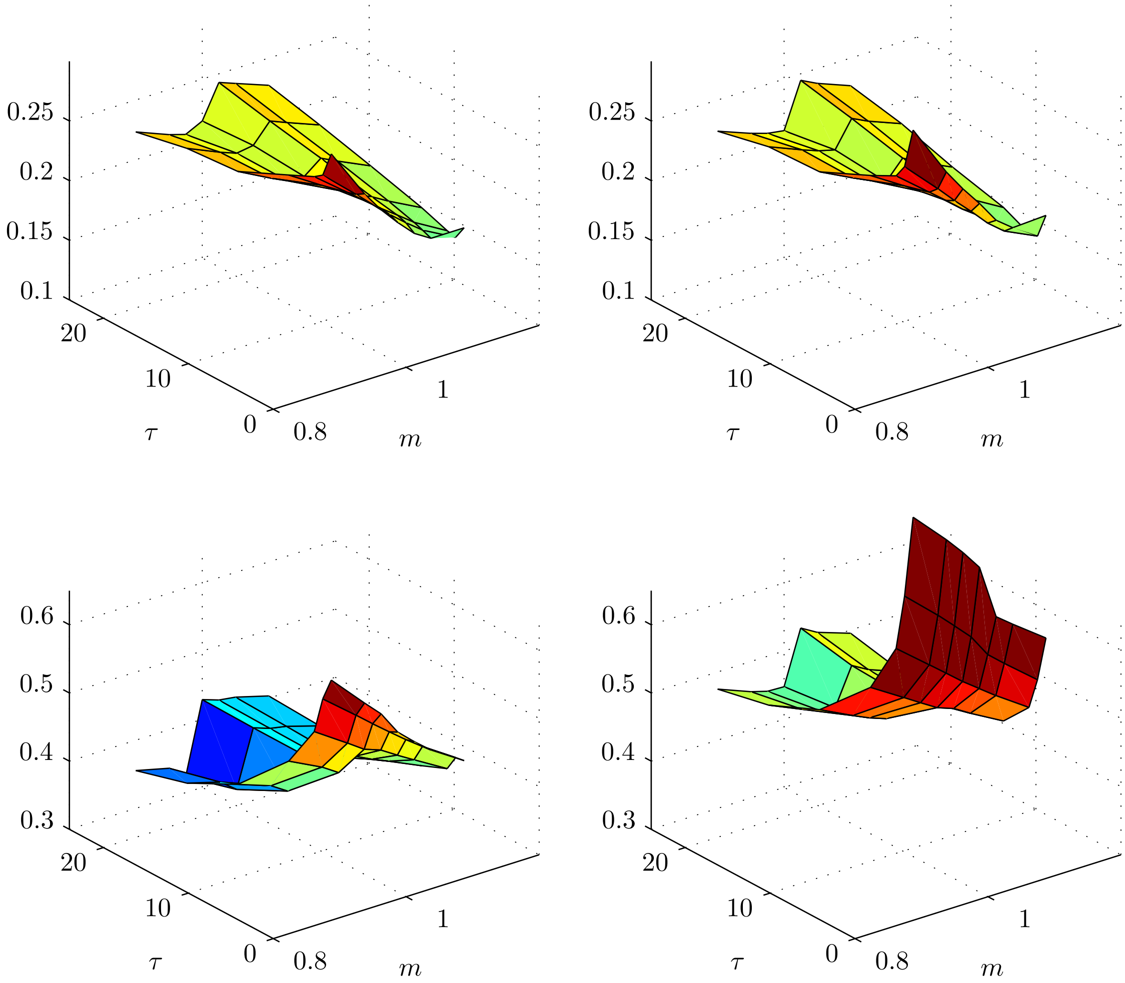

Figure A.6: The implied volatility surface from historical data (left) and the modeled (Benchmark) implied volatility surface (right) of the SX5E index, at July 2008 (top) and October 2008 (bottom). July 2008 has the best fit, while October 2008 has the worst fit.

Heston

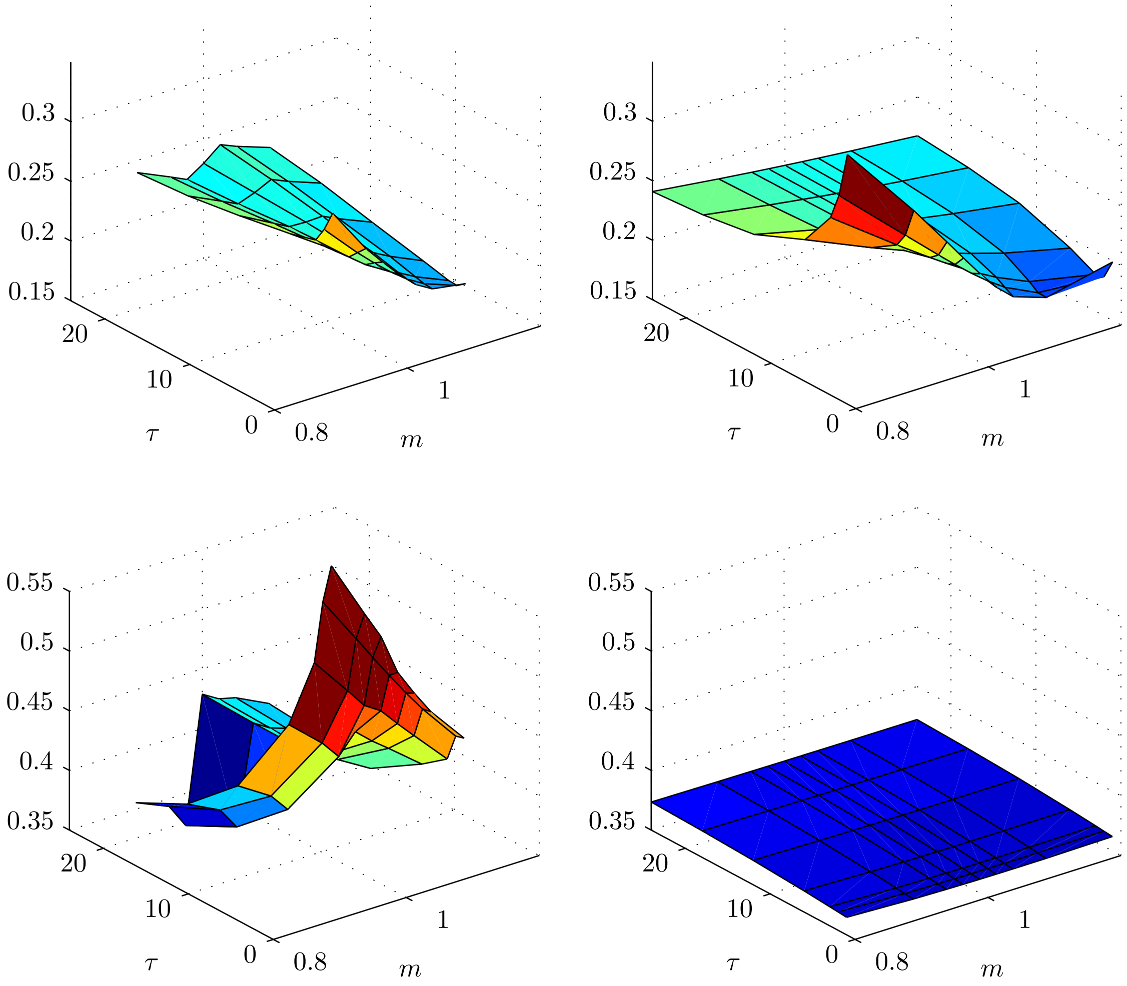

Figure A.7: The implied volatility surface from historical data (left) and the modeled (Heston) implied volatility surface (right) of the SX5E index, at February 2010 (top) and October 2008 (bottom). February 2010 has the best fit, while October 2008 has the worst fit.

PCA

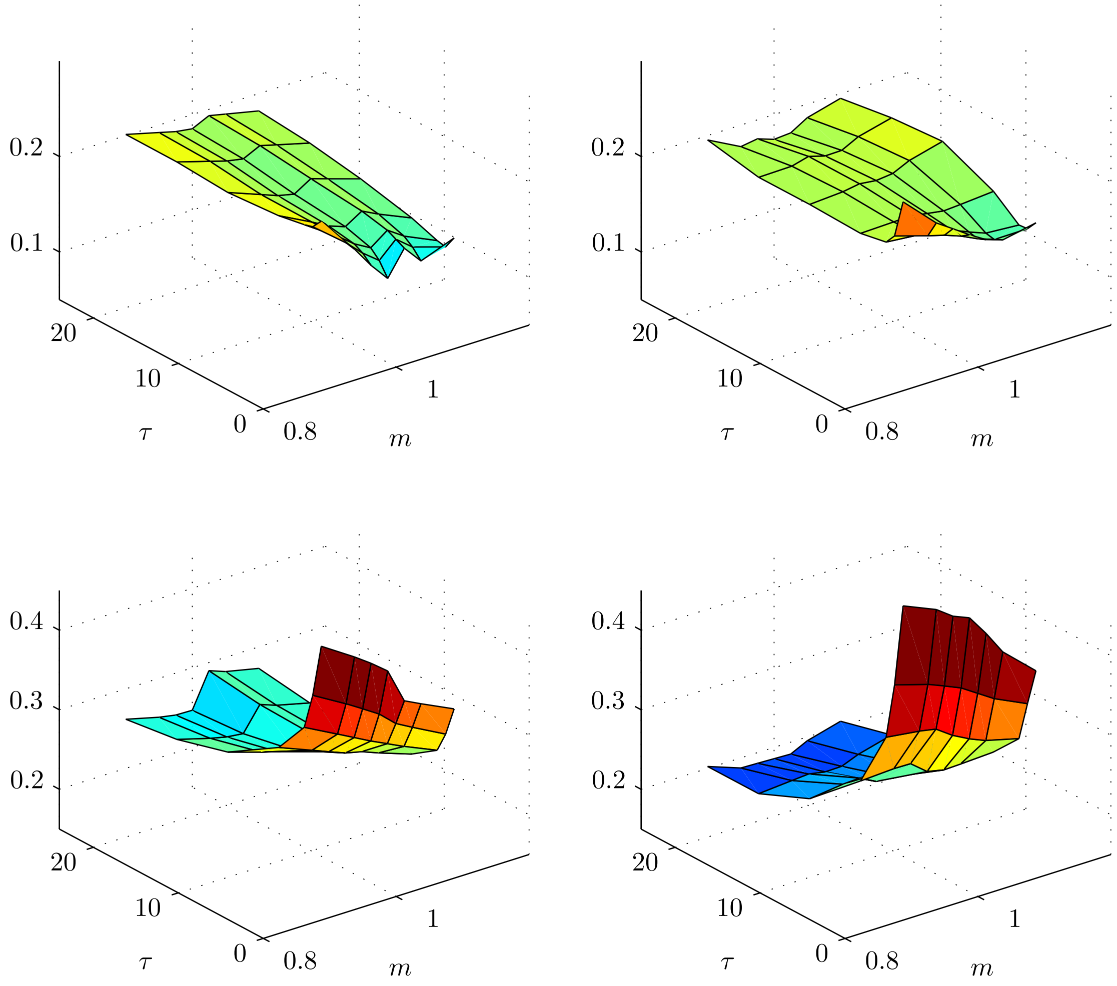

Figure A.8: The implied volatility surface from historical data (left) and the modeled (PCA) implied volatility surface (right) of the SX5E index, at June 2007 (top) and September 2008 (bottom). June 2007 has the best fit, while September 2008 has the worst fit.

Regression

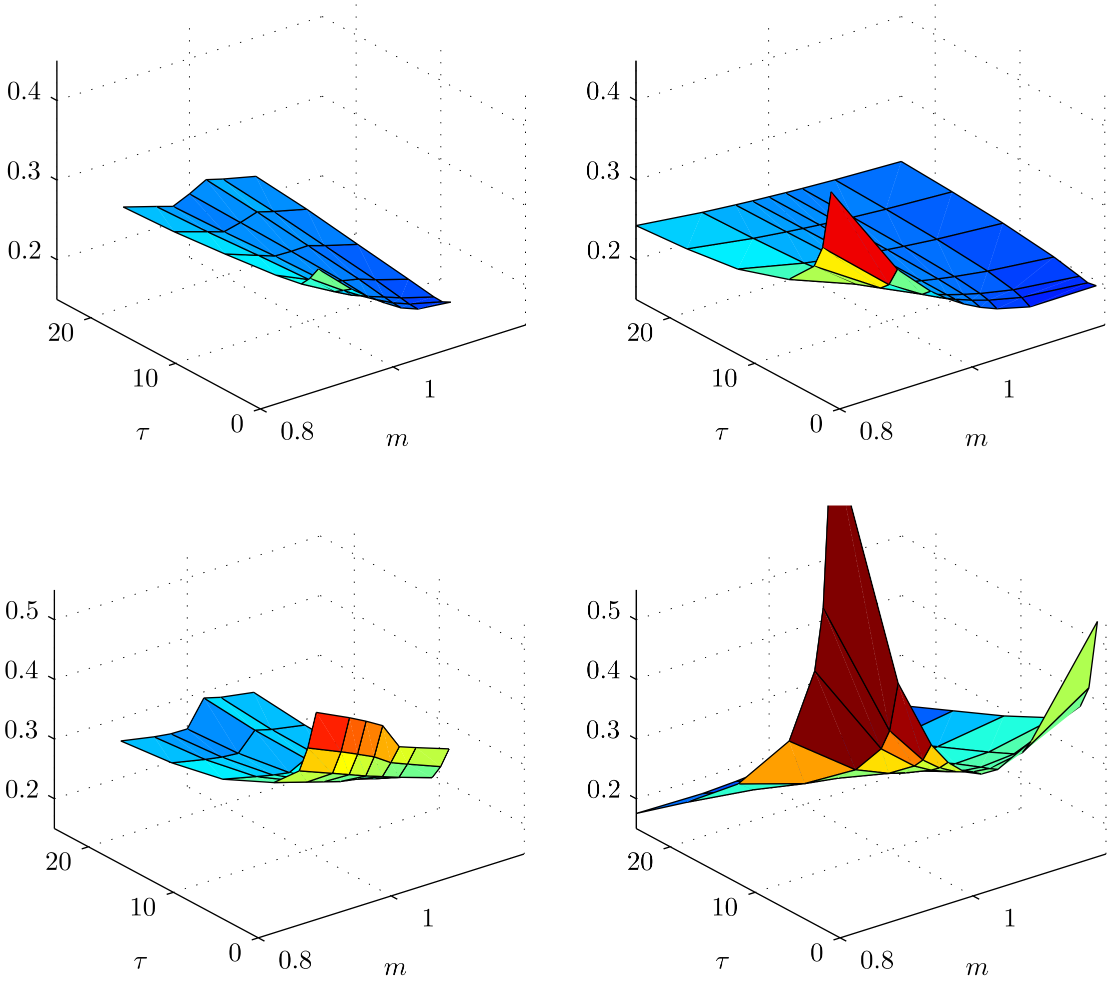

Figure A.9: The implied volatility surface from historical data (left) and the modeled (Regression) implied volatility surface (right) of the SX5E index, at February 2010 (top) and September 2008 (bottom). February 2010 has the best fit, while September 2008 has the worst fit.